Journal of Hydrology: Regional Studies 42 (2022) 101130

Contents lists available at ScienceDirect

Journal of Hydrology: Regional Studies

journal homepage: www.elsevier.com/locate/ejrh

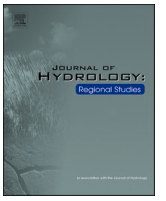

Potential hydro-meteorological impacts over Burundi from climate change

M. Rocío Rivas-López [a,*], Stefan Liersch [a], Christoph Menz [a], Stefan Lange [a], Fred F. Hattermann [a]

[a] Potsdam Institute for Climate Impact Research (PIK), RD2 Climate Resilience, Telegrafenberg A31, 14473 Potsdam, Germany

ARTICLE INFO

Keywords:
Burundi
Climate change
CORDEX
Extremes
Impacts on hydrology
SWIM

ABSTRACT

Study region: Burundi is one of the poorest countries in the world and hence very vulnerable to climate change. It is covered by the Kagera, Malagarasi, and Tanganyika River basins.
Study focus: We investigated the hydro-climatic impacts of climate change over Burundi projected by an ensemble of 19 regional climate models and an eco-hydrological model in two future periods under the RCPs 4.5 and 8.5.
New hydro-climatic Insights: We found a robust increase in annual and seasonal average temperature over Burundi in all scenarios, characterized by a significant annual rising trend along the 21st century and the increase in every single month, especially in the dry season (up to 5.2 °C under RCP8.5-P2). Precipitation would increase in the north, except in February and September. In the south, precipitation would decrease throughout the year, particularly in the onset and offset of the rainy season and from December to February. This would entail the prolongation and severity of the long and short dry periods. These changes generate increases in the long-term annual mean discharges in North Burundi (up to 44% in small catchments and 29% in larger ones). In southern Burundi the discharge would decrease along the year (up to −16.8%) with exception of November-December in the southeast (up to 27.9%). Besides, the higher daily extreme river discharges found over the Ruvubu basin imply a higher risk of floods.

1. Introduction

Climate change does not affect all people equally. Existing and new risks induced by climate change are generally greater for disadvantaged people (IPCC, 2014) like those facing poverty and food insecurity.

Burundi is one of the poorest countries in the world with about 65% of the population living below the poverty line (FAO-UN, 2020). Importantly, the country suffers from alarming food insecurity: almost one in two households (around 4.6 million people) are food insecure (IFRC, 2019) and about 56% of children suffer from chronic malnutrition. There is very limited access to water and sanitation and less than 12% of the population has access to electricity (World Bank, 2022). Most of Burundians (90%) rely on

Abbreviations: CORDEX, Coordinated Regional Climate Downscaling Experiment; SWIM, Soil and Water Integrated Model; BA, Bias adjustment; P1, Period 1; P2, Period 2; LTB, Lake Tanganyika Basin; MRB, Malagarazi River Basin; KRB, Kagera River Basin; kag, Kagera River; mal, Malagarasi River; tan, Tanganyika Lake.

* Corresponding author.
E-mail addresses: rivas@pik-potsdam.de (M.R. Rivas-López), liersch@pik-potsdam.de (S. Liersch), christoph.menz@pik-potsdam.de (C. Menz), slange@pik-potsdam.de (S. Lange), hattermann@pik-potsdam.de (F.F. Hattermann).

https://doi.org/10.1016/j.ejrh.2022.101130
Received 7 July 2021; Received in revised form 1 June 2022; Accepted 3 June 2022
Available online 11 July 2022

subsistence agriculture (FAO-UN, 2020), which counts barely with irrigation (Niyongabo, 2018) and is insufficient to cover household demand.

Burundi has sufficient rainfall with an annual average ranging from 700 to 2000 mm/year; however, its distribution is uneven in space and time and due to its high population density, the country is experiencing increasing pressure on water, soil and land resources (Global Water Partnership, 2011). Additionally, conflict for land emerges since the economic policy does not allow for the equitable distribution of resources (Kamungi et al., 2005).

The high dependence of Burundians on agriculture makes them extremely sensitive to climate variability and extremes. Nationwide famines recorded in the 20th century and regionally in 1989–1990, 2000–2005, and 2008–2010, were the results of extremely dry weather events (FAO-UN, 2016). Moreover, many people were affected by heavy rains, strong winds, floods, and related landslides along the period 1989–2015 (World Bank, 2022). Recently, in 2015–2016, about 90,000 people were affected by El Niño (heavy rains, strong winds) followed by La Niña (late, irregular and insufficient rainfall). These events led to conflicts and internal displacements due to food insecurity. In 2019, almost 80% of the displacements within Burundi were caused by natural disasters (IOM, 2019).

Over the 21st century, temperature is projected to globally rise as well as the frequency and severity of extreme weather events (IPCC, 2014), with Africa likely being the most affected continent (Niang et al., 2015). Therefore, due to Burundi's high vulnerability and dependence on climate variability, it is very important to provide detailed information about the potential impacts of climate change to enhance adaptation options and preparedness (IPCC, 2014). In addition, the Sustainable Development Goals (SDGs) highlight the need to end poverty in all forms and dimensions by 2030, which involves targeting the most vulnerable and supporting communities affected by climate-related disasters. To reach this goal, developing countries must prepare to cope with the impacts of climate change and manage their water resources efficiently, which is key for guaranteeing food resources and human security.

There is little information about the hydrological impacts of climate change in Burundi. Previous research within the White Nile River has paid high attention to Lake Victoria (Sene et al., 2001; Phoon et al., 2004) due to its socioeconomic importance as a source of drinking water. Such studies relate mainly to the change in precipitation over the lake (Thiery et al., 2015, 2016), its water level (Tungaraza et al., 2012), or the stratification (Tierney et al., 2010). Yet, information about the responses in upstream basins, as represented by Burundi's network, is scarce (Kim et al., 2021; Ogiramoi Nyeko, 2011). One reason could be the difficulty to model this area due to the multiple swamps and high evaporation (Di Baldassarre et al., 2011). Moreover, the lack of investment in Burundi due to the violence and conflict in the country since its independence in 1962 (Kamungi et al., 2005), has probably contributed to the research gap in this region Information about climate projections in Burundi can be only found in few publications (Baramburiye et al., 2013; Kim et al., 2021) or extracted from regional maps that illustrate such in Central/East Africa (Endris et al., 2013, 2019; Nikulin et al., 2012); hence lacking accuracy. Despite the existence of a few national plans for adaptation to climate change (NAPA, 2007), the information about climate change impacts is not very detailed.

Climate impact assessments on hydrology normally use Atmosphere-Ocean General Circulation Models, so called Global Climate Models (GCMs), and Regional Climate Models (RCMs). RCMs have been proved to add value to the projections from GCMs by reflecting the effects of local topographic or land feedback with the atmosphere that GCMs are not able to capture due to their lower spatial resolution (Giorgi et al., 2009). Souverijns et al. (2016) found that 77% of the drivers of future precipitation over East Africa can be explained by local or mesoscale feedback and changes in moisture influx, while 23% can be explained by the frequency of occurrence of circulation patterns. Even, some RCMs have been found to derive different climate signs in projected precipitation than their driving GCMs due to their better representation of physical processes (e.g. Saeed et al., 2004, Dosio et al., 2019).

The Coordinated Regional Climate Downscaling Experiment initiative (CORDEX) provides high-resolution regional climate projections (Endris et al., 2013) based on a set of global model simulations in support of the IPCC Fifth Assessment Report (Giorgi et al., 2009). The ability of the CORDEX models to reproduce the characteristics of rainfall patterns at different scales over Africa as well as the influence of the large-scale climate circulation patterns on regional rainfall (teleconnections) has been proven in several studies (Endris et al., 2013, 2016; Nikulin et al., 2012).

Therefore, given the added value of RCMs over GCMs and the ability of the CORDEX RCMs to represent the climate in Africa at a finer scale, the models from the CORDEX initiative have been used in this study as input to a semi-distributed eco-hydrological model to assess future changes in river discharge and water availability in Burundi.

To provide more insights on climate change impacts in Burundi, we (1) evaluated the representation of temperature and precipitation by bias-adjusted CORDEX projections, (2) analyzed the future variation and spatial distribution of average climate variables, and (3) investigated the impact of climate change projections on average and extreme flow regimes in three river basins. Additionally, with this study we intent to provide potential recommendations that may help environmental managers and policy-makers to develop tools to adapt to anthropogenic climate change in Burundi.

2. Materials and methods

2.1. Study area

Burundi is a landlocked country in East Africa covering an area of 27,834 km^2 (Fig. 1). It is located south of the Equator, between the latitudes 1.19°S and 4.27°S and the longitudes 29.00°E and 30.51°E. The country, in the heart of Africa's Great Rift Valley, presents a diverse topography, characterized by five zones. These are the western plain (775–1000 m.a.s.l.), which contains Lake Ruzizi, its wetlands, and Lake Tanganyika; the mountain range "Crête Congo-Nile" that crosses the central-western area from north to south with altitudes reaching 2670 m.a.s.l. (Mount Heha); the central meseta (1400–2000 m.a.s.l.), the depression of Kumoso in the south-east (1200–1400 m.a.s.l.), and the depression of Bugesera in the north-east (1200–1500 m.a.s.l.).

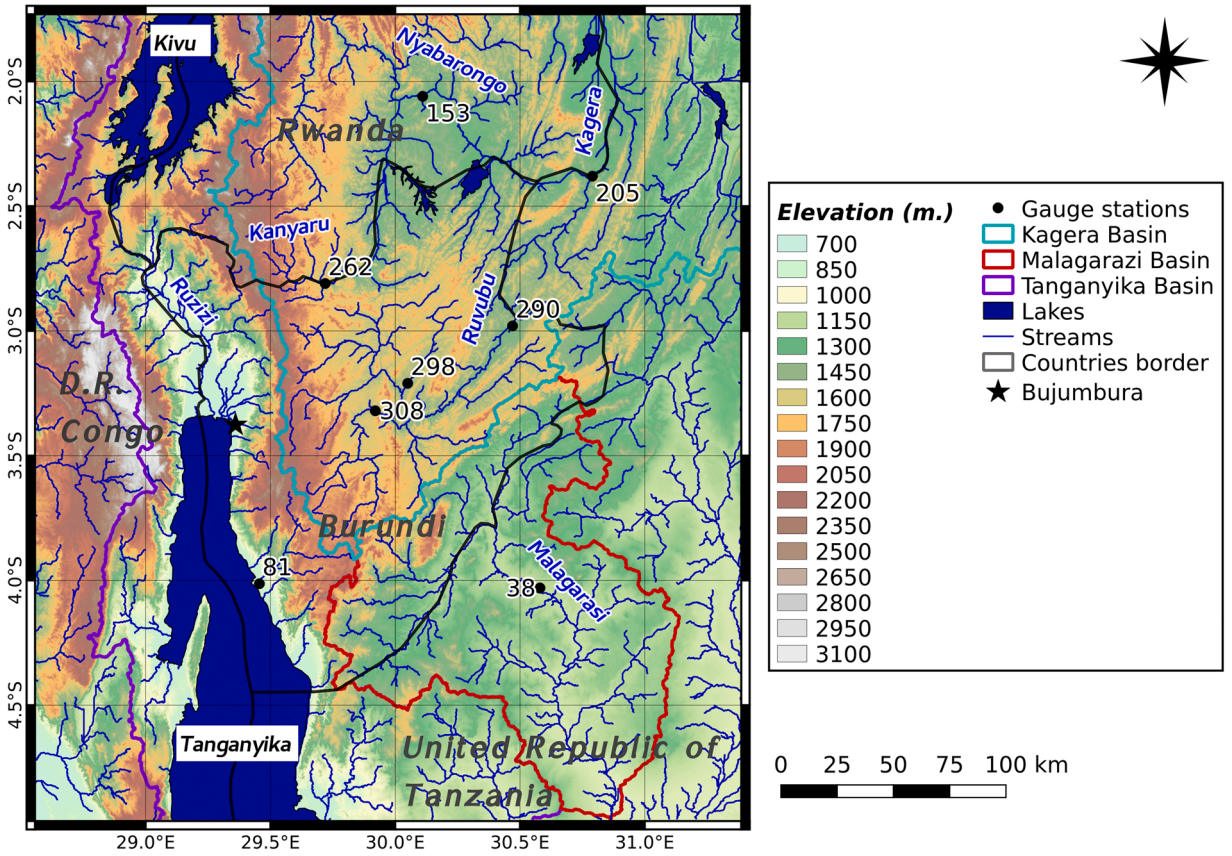

Fig. 1. Map of Burundi, including river basins and gauge stations.

To better analyze and explain spatial differences of climate change in Burundi, the region was split in the following domains: eastern (30.0°E - 31.0°E, 2.5°S - 4.0°S), western (29.0°E - 30.0°E, 2.5°S - 4.0°S), northern (29.5°E - 31.0°E, 2.0°S - 3.5°S and 29.0°E - 29.5°E, 2.5–3.0°S), and southern (29.0°E - 30.5°E, 3.5°S - 4.5°S and 29.0°E - 29.5°E, 3.0°S - 3.5°S), which are shown in Fig. A.2d, b, and c.

2.1.1. Climate

The climatology in the country follows a bimodal pattern with a dry season from June to September and a rainy season from September to May. However, due to the movement of the Intertropical Convergence Zone (ITCZ) the wet season is formed by the "short rains" period that goes from September to December, the "long rains" period from mid-February or March to May, and a short dry season with frequent dry spells in between (ICPAC, 2009; Nkunzimana et al., 2019).

Besides, the variability of the precipitation and temperature in Burundi is strongly related to the altitude (NAPA, 2007; Nkunzimana et al., 2019). Consequently, the Congo-Nile mountain range receives the highest rainfall amounts between 1500 and 2000 mm and experiences the lowest mean temperatures of 14–15°C. In the oriental plains (Bugesera and Kumoso) annual rainfall ranges between 750 and 1250 mm and annual mean temperatures between 20 and 22°C. In the occidental plain (Imbo plain), annual mean precipitation values are between 800 and 950 mm with annual mean temperatures above 23°C. In the occidental escarpment of Mumirwa, precipitation values range from 1000 to 1400 mm per year and annual mean temperatures between 18 and 28°C, whereas in the central high plains, the annual average precipitation ranges between 1200 and 1500 mm and the annual mean temperature is between 17 and 20°C (Sunzu Ntigambirizwa and Ngenzebuhoro, 2009).

2.1.2. Hydrology

The rivers of Burundi (Fig. 1) belong to three main basins: the Tanganyika, Kagera, and Malagarasi River basins. At the same time, the Kagera River belongs to the Nile Basin, while the other two belong to the Congo Basin region.

The (A)kanyaru River flows along the northern border of Burundi with Rwanda, where it joins the Nyabarongo River (Rwanda). The Ruvubu River drains the central part of Burundi and converges into the Nyabarongo River at the Rusumu falls, where the Kagera River starts. The Ruzizi River, which flows along the D.R. Congo-Rwanda-Burundi border and drains into Lake Tanganyika, and the Malagarasi River (South-East Burundi) belong to the Congo River Basin. All the Burundian river basins are trans-boundary.

Table 1
CORDEX models used in this study. Below, the institution responsible for each RCM.

GCM (10)	RCM (5)	Acronym
CCCma-CanESM2	SMHI-RCA4	CanESM2_RCA4
CNRM-CERFACS-CNRM-CM5	CLMcom-CCLM4–8–17	CNRM-CM5_CCLM
CNRM-CERFACS-CNRM-CM5	SMHI-RCA4	CNRM-CM5_RCA4
CSIRO-QCCCE-CSIRO-Mk3–6–0	SMHI-RCA4	CSIRO- Mk3_RCA4
ICHEC-EC-EARTH	CLMcom-CCLM4–8–17	EC-EARTH_CCLM
ICHEC-EC-EARTH	DMI-HIRHAM5	EC-EARTH_HIRHAM5
ICHEC-EC-EARTH	KNMI-RACMO22T	EC-EARTH_RACMO
ICHEC-EC-EARTH	MPI-CSC-REMO2009	EC-EARTH_REMO
ICHEC-EC-EARTH	SMHI-RCA4	EC-EARTH_RCA4
IPSL-IPSL-CM5A-MR	SMHI-RCA4	IPSL_RCA4
MIROC-MIROC5	SMHI-RCA4	MIROC5_RCA4
MOHC-HadGEM2-ES	CLMcom-CCLM4–8–17	HadGEM2_CCLM
MOHC-HadGEM2-ES	KNMI-RACMO22T	HadGEM2_RACMO
MOHC-HadGEM2-ES	SMHI-RCA4	HadGEM2_RCA4
MPI-M-MPI-ESM-LR	CLMcom-CCLM4–8–17	MPI-ESM-LR_CCLM
MPI-M-MPI-ESM-LR	MPI-CSC-REMO2009	MPI-ESM-LR_REMO
MPI-M-MPI-ESM-LR	SMHI-RCA4	MPI-ESM-LR_RCA4
NCC-NorESM1-M	SMHI-RCA4	NorESM1-M_RCA4
NOAA-GFDL-GFDL-ESM2M	SMHI-RCA4	GFDL-ESM2M_RCA4

RCM	Institution
CLMcom-CCLM4–8–17	Climate Limited-area Modeling Community (CLM-Community)
DMI-HIRHAM5	Danish Meteorological Institute
KNMI-RACMO22T	Royal Netherlands Meteorological Institute
MPI-CSC-REMO2009	Helmholtz-Zentrum Geesthacht, Climate Service Center, Max Planck Institute for Meteorology
SMHI-RCA4	Swedish Meteorological and Hydrological Institute, Rossby Centre

2.1.3. Population

Burundi has 11.89 million inhabitants and counts with one of the highest population densities (413 inhab./km^2) and growth rates (3.1%) in the world (World Bank, 2022). The population distribution is very diverse across the country, and ranges between 20 and 8500 inhab./km^2 (the latest is given in the capital city - Bujumbura).[1]

2.1.4. Agriculture

Burundi's economy relies heavily on the agricultural sector, which despite the scarce arable land, employs 80% of the population. 90% of the population depends directly or indirectly on this sector, which is mainly rain-fed (Baramburiye et al., 2013).

2.2. Climate data

2.2.1. WATCH Forcing Data ERA-40

Daily meteorological data (precipitation, minimum, mean, and maximum temperature, solar radiation, and relative air humidity) on a half a degree grid from the Integrated Project Water and Global Change (WATCH) were used as reference (1970–1999) to adjust the bias of the CORDEX models (see section 2.2.3.1) and to calibrate and validate the eco-hydrological model.

As described by Weedon et al. (2011), WATCH Forcing data (WFD) was created for 1958–2001 based on the 40-year ECMWF Re-Analysis product (ERA-40) to be used with land surface and hydrological models. The WFD-ERA40 data were interpolated bilinearly to 0.5° resolution, corrected by elevation and monthly observations of temperature and cloud cover from the Climatic Research Unit (CRU) and precipitation from the Global Precipitation Climatology Centre (GPCC), combined with adjustments for atmospheric aerosol-loading and precipitation gauge corrections for rainfall and snowfall.

2.2.1.1. Performance of WFD-ERA40. The performance of WFD-ERA40 was evaluated based on observed meteorological data from 18 stations across Burundi for seasonal precipitation and near-surface mean temperature in the reference period P0 (1970–1999). Due to the differences in precipitation and temperature patterns in eastern and western Burundi (Fig. A.2d), the evaluation was performed for both regions separately (section 3.1.1). After filling the missing data in the observations (see section 2.2.2 for more information), the meteorological data were interpolated at half-degree resolution by applying the Inverse Distance Weight (IDW) method to be compared with WFD-ERA40. We accounted for the elevation along the Crête Congo-Nile mountain range by specifying a break line within the IDW interpolation.

2.2.2. Observation data

Observed climate data served to check the reliability of WFD-ERA40 (see section 3.1.1). Observed data for precipitation and

[1] https://en.wikipedia.org/wiki/Bujumbura

minimum and maximum temperature were provided for 17 stations within Burundi for (1970–2010) by IGEBU (Geographic Institute of Burundi) via GIZ (Deutsche Gesellschaft für Internationale Zusammenarbeit). We also found meteorological data from IGEBU published on Internet (Simone et al., 2007), and selected precipitation, minimum and maximum temperature for "Kinyinya" station, located in the south-east of Burundi, where we had scarce information.

The observations were not complete, so we filled manually the missing daily data by averaging values from adjacent days when possible. We found years with less than 200 observed daily data and months with less than 15 dis-/continuous daily time steps that we had to discard. Table A.1 shows the percentage of missing data in each station for precipitation, minimum and maximum temperature. More than 70% of the stations show less than 25% missing data.

2.2.3. CORDEX

As climate projections we used in total 19 combinations of 10 driving GCMs and 5 RCMs from the COordinated Regional Downscaling EXperiment (CORDEX[2]) for the Africa CORDEX domain at a resolution of 0.44 degree (AFR-44) in this study. Table 1 summarizes the 19 GCM-RCMs combinations.

Our study focuses on two greenhouse gas concentration scenarios: the "Representative Concentration Pathway (RCP)" 4.5 and 8.5. The lower end concentration scenario RCP 2.6 was excluded due to the insufficient number of available projections when performing this study.

2.2.3.1. Bias adjustment of the CORDEX models. In order to avoid the propagation of the uncertainty/error from the climate models across the impacts modeling chain, all climate projections were bias adjusted prior to run the eco-hydrological model. For it, we used the Inter-Sectoral Inter-Model Intercomparison Project (ISIMIP, www.isimip.org) - ISIMIP3BA method (Lange, 2019). As reference observation dataset and period for the bias adjustment we used WFD-ERA40 and 1970–1999. For this task, the CORDEX data were remapped to a half-degree resolution geographic grid, likewise WFD-ERA40. The ISIMIP3BA bias adjustment method is a quantile mapping method that fits the cumulative distribution function of the target data. It is specifically tailored to reduce the bias in the tails of the distribution (i.e., extremes) while it preserves the trends in each quantile. The bias adjustment was applied separately (univariate) to the variables needed for the hydrological model: precipitation (prec), temperature (tas), relative humidity (hurs), and solar radiation (rsds). For the maximum (tasmax) and minimum (tasmin) temperature, the ISIMIP3BA method derives new values from the bias-adjusted temperature, its range and skewness. Whenever needed we converted the calendars of the CORDEX models to proleptic Gregorian using linear regression of neighboring dates.

2.2.4. Climate scenarios

The RCP 4.5 and RCP 8.5 (Meinshausen, 2011; Moss et al., 2010) were used to explore the change of meteorological variables in two 30-year periods in the 21st century (P1: 2030–2059 and P2: 2069–2098) with reference to the historical period (P0: 1970–1999). The RCP 4.5 represents a medium-low global anthropogenic radiative forcing that gets stabilized, whereas the RCP 8.5 represents high radiative forcing as a result of increasing greenhouse gas emissions over time. These two scenarios allow exploring the impacts of a warming world by providing a wide climate range that includes a "soft mitigation" scenario (RCP 4.5) and the so-called "business as usual" or "unlikely worst case" scenario (RCP 8.5). The far future 30-year period was constraint to 2098 by the HadGEM2-ES model, that provides simulation data until November 2099 for some combinations of RCMs - RCPs.

2.3. Data for hydrological modeling

The data used to set-up, calibrate, and validate the hydrological model are:

- a digital elevation model (DEM) with 3 arc-second resolution (about 90 m at the equator), from the NASA's Shuttle Radar Topography Mission (SRTM) (Jarvis et al., 2008),
- a soil map merged obtained from two sources: the Harmonized World Soil Database v1.2 (Fischer et al., 2008), which is a 30 arc-second raster database, and a more detailed map from the Soil and Terrain database of Central Africa (SOTERCAF, version 1.0), compiled for the Democratic Republic of Congo, Rwanda, and Burundi, counting with 20 soil profiles for Burundi (Van Engelen et al., 2006),
- a land-use map downloaded from the AFRICOVER Project from the Food and Agricultural Organization of the United Nations (FAO), called "Multipurpose Landcover Database for Burundi", at scales 1:250000 and 1:1 million (Kalensky, 1998), counting with until 117 land cover classifiers, later reclassified into the 15 land cover classes supported by the SWIM,
- WFD-ERA40 climate dataset (described in section 2.2.1),
- and daily/monthly observed discharge data for eight gauging stations obtained from IGEBU and the Global Runoff Data Centre (GRDC),[3] for the evaluation of the performance of the hydrological model (section 3.3.1).

[2] https://cordex.org/
[3] http://www.bafg.de/GRDC/EN/Home/homepage_node.html

Table 3
Model evaluation for (a) daily discharge for two stations located within Kagera River Basin and (b) mean monthly streamflow for eight gauge stations in the Kagera River (kag), Malagarasi River (mal), and Tanganyika Lake (tan) basins. *Mean annual streamflow indicated as in the GRDC database (in 2017).

(a) Daily time step										
Station ID	Name	*Q (m^3/s)	Cal. period	NSE	PBIAS	RSR	Val. period	NSE	PBIAS	RSR
kag_308	Ruvyironza-Kibaya	23.69	1975–1983	0.49	− 6.9	0.71	1984–1994	0.52	− 10.1	0.69
kag_290	Muyinga	95.94	1975–1983	0.44	− 10.8	0.75	1984–1993	0.45	1.6	0.74
(b) Monthly time step										
Station ID	Name	*Q (m^3/s)	Cal. period	NSE	PBIAS	RSR	Val. period	NSE	PBIAS	RSR
kag_153	Kanzenze	109.33	1970–1978	0.68	− 0.3	0.56	1979–1984	0.58	1.3	0.64
kag_262	Ngozi-Butare	22.92	1975–1984	0.61	− 11.8	0.62	1985–1991	0.82	3.5	0.42
kag_298	Ndurumu-Shombo	n.a.	1975–1983	0.7	0.6	0.55	1984–1999	0.52	2	0.69
kag_308	Ruvyironza-Kibaya	23.69	1975–1983	0.71	− 1.2	0.53	1984–1994	0.76	− 7.9	0.49
kag_290	Muyinga	95.94	1975–1983	0.71	− 10.5	0.54	1984–1993	0.66	1.8	0.58
kag_205	Rusumo	224.06	1970–1977	0.63	− 2.3	0.61	1978–1984	0.58	0.2	0.65
mal_38	Taragi road bridge	68.01	1972–1976	0.72	− 12.5	0.52	1977–1979	0.73	19.6	0.51
tan_81	Basse-Mutambara	17.94	1981–1986	0.60	9.3	0.63	1987–1989	0.78	− 8.6	0.46

2.4. Hydrological model

The Soil and Water Integrated Model (SWIM) is a semi-distributed eco-hydrological model developed at the Potsdam Institute for Climate Impact Research (PIK), based on the previously developed models SWAT (Arnold et al., 1993) and MATSALU (Krysanova et al., 1989). It operates on a daily time step and uses a 3-level dis-aggregation scheme: basin - subbasin - hydrotope or Hydrological Response Unit (HRU), defined as the smallest unit that belongs to the same subbasin, characterized by the same soil and land use type, and therefore presenting the same hydrologic behavior. Additional information about SWIM, its characteristics, applications, and performance can be found in Krysanova et al. (1998, 2015).

SWIM was set-up independently for the three river basins within Burundi: Kagera River Basin (KRB), Malagarasi River Basin (MRB), and Lake Tanganyika Basin (LTB). The minimum sub-basin area was 50 km^2. SWIM, driven by WFD-ERA40, was calibrated and validated with daily and monthly river discharge, according to the available observed discharge data, for eight gauge stations (Fig. 1) under different time frames (see table 3). The calibration was performed manually in a first step and then optimized using the automated algorithm PEST,[4] a software for model-independent parameter estimation and uncertainty analysis. The representation of small lakes and wetlands was included indirectly within the parametrization of the model through e.g. higher delay applied to sub-surface and groundwater flow, or the correction of the saturated conductivity and curve number of the soils.

The performance of discharge simulations was evaluated using three common indicators, the Nash-Sutcliffe efficiency (NSE; Nash and Sutcliffe, 1970), the percent bias (PBIAS), and the ratio of the Root Mean Square Error (RMSE) to the standard deviation of the observations (RSR; Moriasi et al., 2007).

2.5. Indicators of climate change

We used the following indicators for the evaluation of the hydro-meteorological impacts of climate change in Burundi:

- long-term annual and monthly mean precipitation and near-surface temperature over Burundi.
- long-term annual and monthly mean river discharge, calculated as the 30-year averages of daily sums.
- daily low (Q90, Q95, and Q99) and high (Q10, Q5, and Q1) flows over 30-year periods. Q10 is the discharge that is equaled or exceeded 10% of the flow record, idem for the rest.

2.5.1. Averages

The climatic changes over Burundi were computed as the fractional percent coverage by multiplying the 0.5° gridded climate data by a mask,[5] indicating the area percentage covered by the country for each grid cell (see Fig. A.2a), obtained from ISIMIP. Averages over the full domain are calculated over the rectangle covering the area between (28.0°E, 5.5°S) and (32.0°E, 1.0°S). For the comparison of WFD-ERA40 with observed data, we calculated the long-term monthly mean averages for the east and west of Burundi (Fig. A.2d), while the anomalies in the future were calculated as the fractional coverage over the northern (Fig. A.2b) and southern (Fig. A.2c) regions of Burundi. Such domains were defined by the pixels indicating opposite sign of change.

[4] http://www.pesthomepage.org
[5] https://gitlab.pik-potsdam.de/isipedia/countrymasks/blob/master/countrymasks_fractional.nc

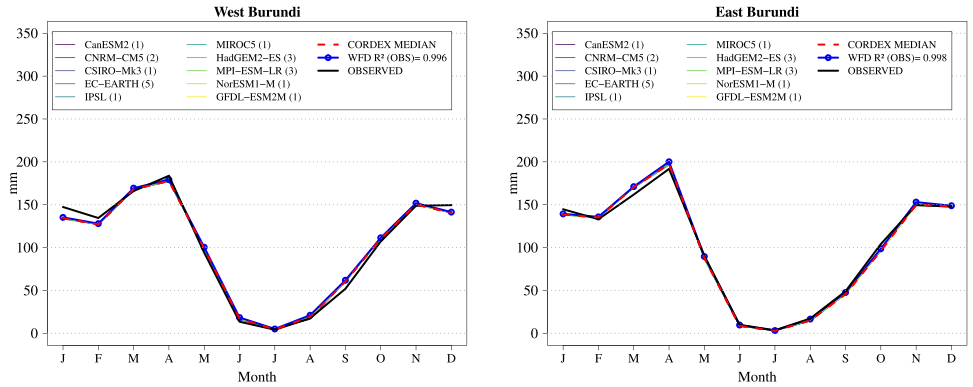

(a) Long-term monthly mean precipitation

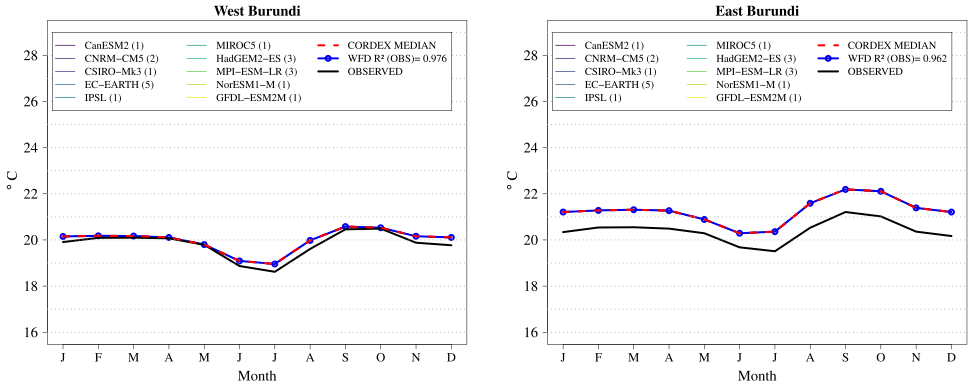

(b) Long-term monthly mean temperature

Fig. 2. Comparison of seasonal climate in the reference period P0 (1970–1999) in East and West Burundi between WFD-ERA40 and observed data, and bias-adjusted projections from CORDEX models for the same period, averaged by GCM. The CORDEX projections are non visible since they match WFD-ERA40 data. The number of RCMs driven by each GCM is indicated in the legend, between brackets. The CORDEX ensemble median was calculated over 19 GCM-RCM combinations. The correlation between WFD-ERA40 and the observations is given in the legend as WFD R^2 (OBS).

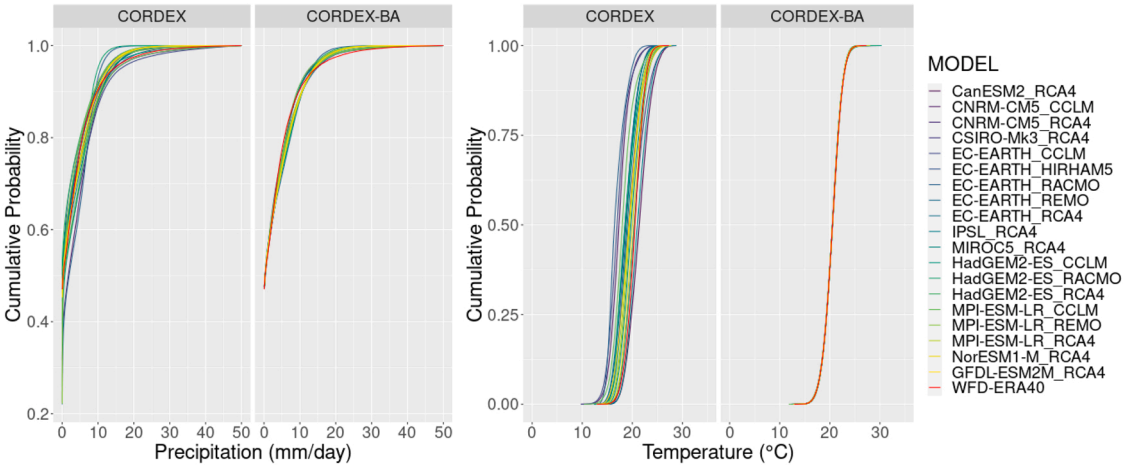

(a) Precipitation (the range of the values in the x axis has been limited to [0,50])

(b) Average near-surface average temperature

Fig. 3. Cumulative Distribution Function (CDF) of daily precipitation and mean temperature values for 19 CORDEX GCM-RCM combinations before and after bias adjustment (here named as CORDEX and CORDEX-BA respectively), and WFD-ERA40.

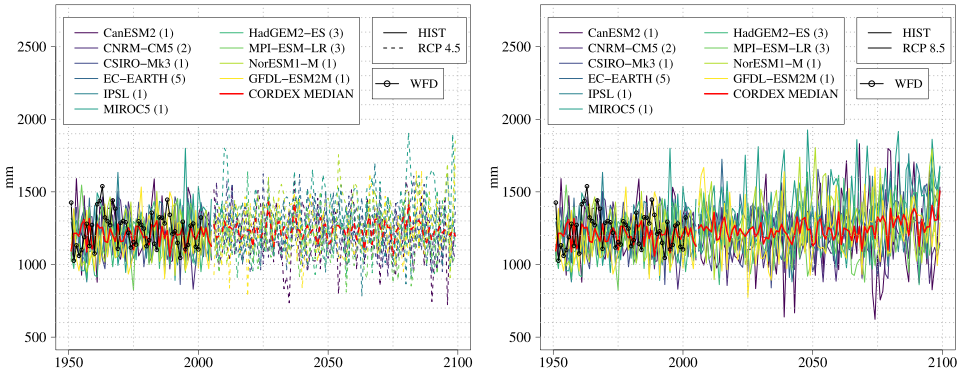

(a) Annual precipitation in the north of Burundi for the historical scenario and RCP 4.5

(b) Annual precipitation in the north of Burundi for the historical scenario and RCP 8.5

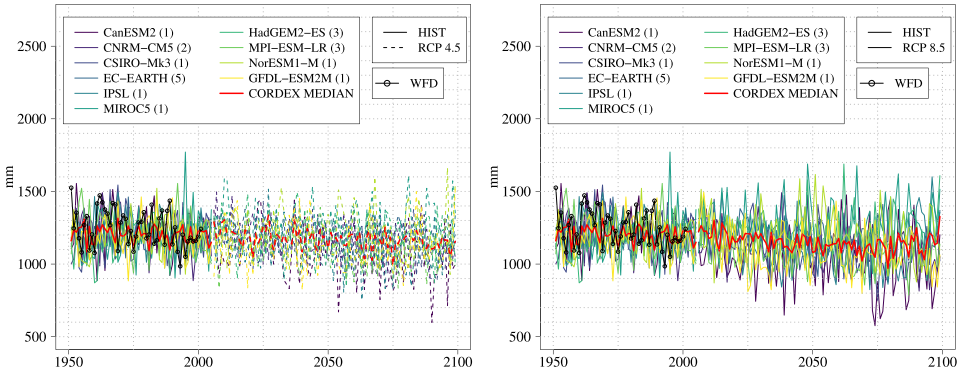

(c) Annual precipitation in the south of Burundi for the historical scenario and RCP 4.5

(d) Annual precipitation in the south of Burundi for the historical scenario and RCP 8.5

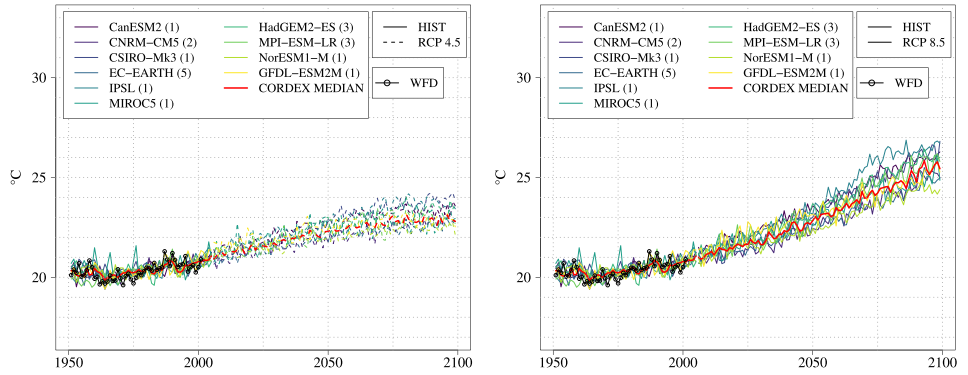

(e) Annual temperature averaged over Burundi for the historical scenario and RCP 4.5

(f) Annual temperature averaged over Burundi for the historical scenario and RCP 8.5

Fig. 4. Annual total precipitation and mean surface air temperature from WFD-ERA40 for the past period (1951–2001) and CORDEX projections (averaged by GCM) for the historical scenario (1951–2005) and under RCPs 4.5 and 8.5 (2006–2099). The number of RCMs driven by each GCM (average of RCMs) is indicated in the legend, between brackets. The CORDEX ensemble median was calculated over 19 GCM-RCM combinations.

3. Results

3.1. Past climate

3.1.1. Past climate represented by WFD-ERA40

In this section, we analyze how long-term annual mean temperature and precipitation are represented by WFD-ERA40 over

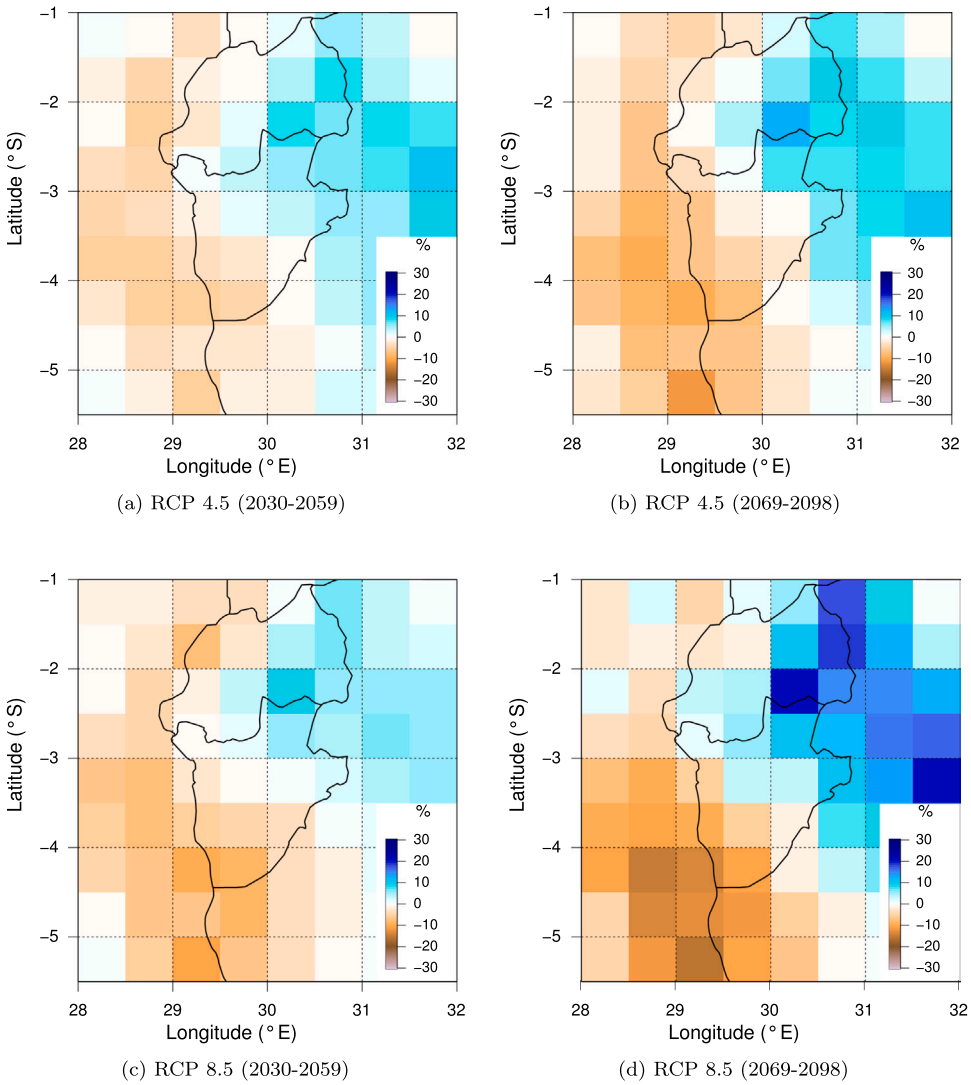

Fig. 5. Spatial changes in average annual mean precipitation projected by the median of CORDEX models.

Burundi in the reference period P0 (1970–1999), compared to the observations.

The spatial distribution and value ranges indicated by WFD-ERA40 agree with the climate described in national reports (Sunzu Ntigambirizwa and Ngenzebuhoro, 2009) and with observed meteorological data.

The correlation of seasonal mean precipitation and temperature for East and West Burundi between WFD-ERA40 and observed meteorological data shows a very good fit with R^2 above 0.99 (Fig. 2). WFD-ERA40 indicates slight deviations from the observations for seasonal mean precipitation during the rainy season (December-February in West Burundi and in March and April in the east). On the other side, WFD-ERA40 overestimates mean air temperature by less than 0.4°C in West Burundi and about 1°C or less in the eastern part. These differences could probably be due to the interpolation applied to the observed data, since the IDW method does not take into account for the elevation of the stations.

Despite some differences, due to the good fit of the long-term monthly mean temperature and precipitation data, its temporal continuity, and the availability of more climate variables than in the observed data, WFD-ERA40 was used as meteorological input to calibrate and validate SWIM and to adjust the bias of the CORDEX projections with reference to P0 (1970–1999).

3.1.2. Past climate represented by CORDEX

The Cumulative Distribution Function (CDF) of daily precipitation and temperature values simulated by 19 CORDEX models before and after adjusting the bias to WFD-ERA40 in 1970–1999 with the ISIMIP3BA method (see section 2.2.3) can be seen in Fig. 3.

A significant improvement can be observed in the distribution of the daily precipitation in the CORDEX data after bias-adjustment (CORDEX-BA) (Fig. 3a) like for instance in the lower and higher tails of the distribution: the number of dry days in CORDEX-BA has increased from 40% to 48%, similarly than in WFD-ERA40 (47%), and the maximum precipitation value has decreased from 301 mm

Table 2
Changes projected by the CORDEX ensemble median for the long-term annual mean (a) precipitation and (b) temperature for each scenario and period. Average over Burundi (Avg. B), average over the domain (Avg. domain), minimum (Min. B), and maximum (Max. B) values over Burundi, average of the values showing an increase (Avg. + B) and a decrease (Avg. - B) within Burundi, and CORDEX models range over Burundi (Models range B).

(a) Relative changes in precipitation

CORDEX	Precipitation anomalies (%) - CORDEX ensemble median						
Scenario	Avg. B	Avg. domain	Min. B	Max. B	Avg. + B	Avg. - B	Models range B
RCP4.5-P1	1.0	1.1	− 5.4	9.0	2.0	− 1.1	− 20.3, 25.7
RCP4.5-P2	− 1.3	0.2	− 9.1	12.3	1.6	− 2.8	− 30.3, 31.7
RCP8.5-P1	− 1.2	− 0.8	− 9.2	9.8	1.2	− 2.4	− 26.6, 30.7
RCP8.5-P2	0.6	1.4	− 13.4	20.7	3.6	− 3.0	− 48.9, 43.5

(b) Absolute changes for mean air temperature

CORDEX	Temperature anomalies (°C) - CORDEX ensemble median				
Scenario	Avg. B	Avg. domain	Min. B	Max. B	Models range B
RCP4.5-P1	1.8	1.8	1.7	1.8	1.1, 2.3
RCP4.5-P2	2.4	2.4	2.3	2.5	1.6, 3.5
RCP8.5-P1	2.2	2.2	2.0	2.3	1.3, 2.9
RCP8.5-P2	4.3	4.3	4.1	4.4	3.1, 5.9

to 171 mm in CORDEX-BA.

Idem for temperature, Fig. 3b shows that most of the CORDEX models underestimated daily mean values in comparison to WFD-ERA40 before the BA, whereas the new distribution of the CORDEX values after BA fits very good the one from WFD-ERA40.

In the long-term and after the bias adjustment, the monthly average precipitation and temperature of the CORDEX climate data fits perfectly the values from WFD-ERA40 (see after and previous bias correction in Figs. 2 and A.3 respectively).

Regarding the annual values, after the BA, the average of the annual total precipitation shown by the CORDEX ensemble median over the past period (1951–2001) is 2% lower than the WFD-ERA40 average (1242 mm). Most of the single annual values from the GCMs (average of driven RCMs) oscillate between 900 and 1600 mm while the ones from WFD-ERA40 are between 900 and 1538 mm. (Figs. 4a and 4c illustrate the projections in the north and south of Burundi during the historical period). We also found outlying annual precipitation values above 1800 mm. in the north and south of Burundi, projected by MIROC5.

Regarding the annual mean near-surface temperature, according to the Mann-Kendall (MK) test (Mann, 1945), the CORDEX models ensemble median as well as WFD-ERA40 show significant increasing trends. Additionally, Figs. 4e and 4f show that not only the median but all CORDEX GCMs (average of driven RCMs) project steadily increasing temperatures during the past.

3.2. Climate projections

In this section, the changes in the long-term annual and monthly mean precipitation and temperature under the RCPs 4.5 and 8.5, and for the 30-year periods P1 (2030–2059) and P2 (2069–2098) with reference to the period P0 (1970–1999) are reported. In the context of temperature, we report absolute anomalies while for precipitation, we report relative changes.

3.2.1. Annual anomalies

We found a similar spatial pattern of change in the long-term annual average precipitation across all scenarios that divide the whole domain into two parts (Fig. 5): the eastern and central-northern regions showing positive anomalies, and the western and central-southern areas showing negative changes.

This gets translated into a generalized increase of precipitation in the north of Burundi projected by the median of CORDEX models between 1.2% and 3.6% (this is the range of weighted spatial mean for all scenario-periods), reaching higher values under RCP8.5-P2 up to 20.7% in the cell with center in (30.25°E, 2.25°S), and a mean decrease in the south by − 1.1 to − 3%, with maximum values up to − 13.4% in the southwest of Burundi (at 29.25°E, 4.25°S)(see grid cells for the north/south of Burundi in Fig. A.2b and c). The area of Burundi at the north of Lake Tanganyika (pixel with center in (29.25°E, 2.75°S)) and in the cell with center in (29.75°E, 3.25°S) show a decrease of precipitation in RCP4.5-P2 and practically no change in RCP8.5-P1.

The magnitude of change rises gradually from RCP4.5-P1 (Fig. 5a) to RCP 8.5-P2 (see 5d) and geographically: the more to the northeast/southwest of Burundi, the higher the absolute anomalies. Moreover, the values projected by single models are between − 48.9% and 43.5%. The model CNRM-CM5_CCLM projects the minimum anomalies for precipitation in three of the scenarios while MIROC5_RCA4 and EC-EARTH_RACMO are the models projecting the maximum positive changes.

In the long-term, the CORDEX multi-model median projects a significant increasing trend (p-value < 0.05) for annual precipitation after the MK test in the north of Burundi under RCP8.5 (Fig. 4b), and a significant decreasing trend in the south under both RCPs (see 4c and d).

Regarding temperature, all CORDEX models agree on an increase in the long-term annual 30-year average for all scenarios and periods between 1.8°C (RCP4.5-P1) and 4.3°C (RCP8.5-P2) over Burundi (see Table 2b and spatial plots in Figure A.4). The anomalies projected over Burundi remain similar to the average change over the whole domain and do not vary significantly across the country

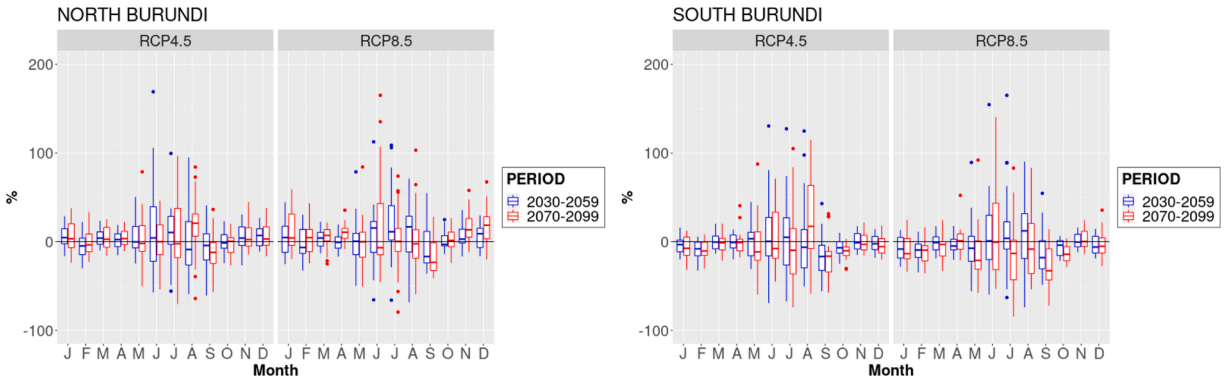

(a) Relative anomalies for precipitation in North and South Burundi (the y axis has been limited to 200%)

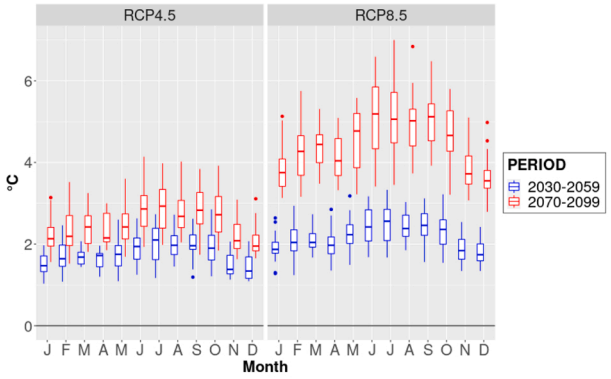

(b) Absolute anomalies for mean temperature over Burundi

Fig. 6. Long-term monthly mean anomalies in precipitation and temperature projected by CORDEX, for RCP4.5 and 8.5, and periods P1 (2030–2059) and P2 (2069–2098), in relation to P0 (1970–1999).

(maximum spatial variation=0.3°C). Moreover, single models project minimum and maximum changes in single cells over Burundi of 1.1°C (RCP4.5-P1) and 5.9°C (RCP8.5-P2).

We also found significant rising trends (p-value = 0.00) in the annual mean temperature projected by the median of the CORDEX ensemble over Burundi, according to the MK test (see Fig. 4e and f), during the historical period (1951–2005), and the future period (2006–2099) under both RCPs: 4.5 and 8.5. These trends result in an approximate increase of 2.7°C under RCP4.5 and 5.3°C under RCP8.5 by the end of 21st century, compared to 1951 (difference between the 5-year average from both time ends).

3.2.2. *Monthly anomalies*

Fig. 6a shows the relative change in long-term monthly average precipitation in North and South Burundi.

According to the CORDEX ensemble median, the precipitation in North Burundi is very likely to increase during both rainy seasons: November-January and March-April, especially in RCP8.5-P2 (up to 10.7% in April, 13.4% in November, and 18.7% in December). CORDEX projects as well a robust increase during the dry season (June-August) mostly in intermediate scenarios (RCP.4.5-P2 or RCP8.5-P1) with significative magnitudes of rise (up to 20.9% in August). On the other side, the CORDEX models (median) project a robust decrease of precipitation in February (except in RCP8.5-P2) and September (up to −23.2%, in RCP8.5-P2). All the anomalies highlighted count with a very high agreement from the CORDEX models (above 78% in most of the cases).

In South Burundi, the multi-model median indicates a general decrease of precipitation along most of the year, with some exceptions found from April to August in different scenario-periods. More robust and meaningful magnitudes of decrease are projected in December-February (with up to −13.5% in January), May (up to −21%) and September-October (with up to −32.8% in September and −14.2% in October), with the largest magnitudes found in RCP8.5-P2. On the other side, the exceptions showing the most significant increments occur in July (up to 5% in RCP4.5-P1) and August (18.8% in RCP4.5-P2 and 12.2% in RCP8.5-P1).

Regarding the long-term monthly mean temperature, there is a unified agreement from the CORDEX models in an increase in every single month, scenario and period. A lower increase is projected over the rainy months (November-April), while a higher increase would take place during the dry season (June-September), extended to May and October. The multi-model median lies between 1.3°C (December, RCP4.5-P1) and 5.2°C (June, RCP8.5-P2).

Table 4
Model evaluation (PBIAS - %) for extreme daily low and high flows (percentiles - Qx) over the calibration and validation periods for two stations.

Station ID	Calibration period	Q99	Q95	Q90	Q10	Q5	Q1
kag_308	1975–1983	23.7	17.6	11.0	− 8.0	− 9.4	− 17.7
kag_290	1975–1983	− 14.7	− 17.6	− 20.6	− 3.5	2.1	− 1.7
Station ID	**Validation period**	**Q99**	**Q95**	**Q90**	**Q10**	**Q5**	**Q1**
kag_308	1984–1994	21.8	14.1	8.4	− 13.1	− 14.8	− 15.5
kag_290	1984–1993	17.7	3.7	− 0.4	11.3	10.6	10.7

3.3. Hydrological processes

3.3.1. Model evaluation

In this section we report the results of the model performance at the daily and monthly time steps. For the daily time step, we show the model rate for the stations for which daily discharge was available and we could success with the calibration and validation in SWIM: kag_308 and kag_290. For monthly mean discharges, we show the model results for eight gauge stations (see Fig. 1): six gauge stations located in KRB, one in MRB and another one in LTB.

At Lake Tanganyika Basin, no observed discharge data was available at the outlet of Kivu Lake (see Fig. 1), and therefore only the calibration of small streams draining into the Lake Tanganyika was possible. The station "tan_81″ was the only one for which the model evaluation was satisfactory within Tanganyika Basin. For other stations measuring discharges flowing into Tanganyika Lake, the resolution of the WFD-ERA40 climate (0.5° x 0.5°), together with the location of the gauge stations in headwater sub-basins, and the small magnitudes of discharge (10–20 m^3/s) routed by those sub-basins, made the calibration of SWIM not possible.

For the daily time step (table 4), we consider our results for kag_308 and kag_290 satisfactory based on the results from the literature presented by Moriasi et al. (2007) but also on the visual comparison of observed and simulated streamflow (Fig. A.5). Thus, it can be seen that SWIM represents well the daily dynamics for average flows for both stations, however for the low and high flows we find considerable over-/underestimation in some years (e.g. for high flows in 1982, 1985, and 1989). Therefore, we also evaluated the model performance for extreme flows for kag_290 and kag_308. Table 4 shows the PBIAS between the observed and simulated annual percentiles of discharge (Qx), calculated over the calibration and validation periods. We consider a good performance for those indicators if the PBIAS is below ± 25%, condition fulfilled for all the percentiles (Q99, Q95, Q90, Q10, Q5, and Q1) for the both stations. Hence, we include the anomalies for these percentiles in the climate impact assessment (Section 3.3.3).

For the monthly time step, according to Moriasi et al. (2007) our results of the model performance (see Table 3b) range from satisfactory ($0.5 < NSE =< 0.65$, $15 =< |PBIAS| =< 25$, and $0.5 < RSR =< 0.6$) to very good ($0.75 < NSE =< 1$, $|PBIAS| < 10$, and $0 =< RSR =< 0.5$). The plots showing the comparison of the observed and simulated monthly and seasonal mean discharges for the calibration and validation periods for each station can be found in the annex (Figs. A.6, A.7, and A.8).

In the monthly plots (Figs. A.6, A.7, and A.8) it can be observed that SWIM simulates properly the flow dynamics in all stations and meet quite well the monthly high and low flows with exception of some peaks (e.g. in 1982 in kag_262, kag_308 and kag_290; 1973 in mal_38, or 1988 in tan_81).

3.3.2. Long-term annual and monthly average discharge anomalies

SWIM projects an increase in the long-term annual average discharge (Fig. 7a) for most of the stations in the Kagera River Basin (KRB), under both RCPs and for both future periods, according to the median of the simulations driven by CORDEX, with exception of kag_308 (station covering the streamflow from the mountainous area in central-southern Burundi) that shows a decrease, and kag_290 in RCP8.5-P1 showing no change. The stations showing a greater increment in discharge are the ones located northwards of the study area, according to the higher rise found for precipitation (see Section 3.2.1). The changes indicated by the median of the CORDEX models for each station (in descending order) are: kag_298, which registers increases in the Ndurumu River (tributary of the Ruvubu River) ranging from 7.2% (RCP8.5-P1) to nearly 44% (RCP8.5-P2), kag_153, located in Rwanda, that shows increases going from 11.8% (RCP4.5-P1) to 29.0% (RCP8.5-P2), kag_205 that registers an increase from nearly 11% (RCP4.5-P1) to 23.5% (RCP8.5-P2), and kag_262 showing an increment between 6.8% (RCP4.5-P1) and 16.6% (RCP8.5-P2). Additionally to these stations, kag_290, which drains the main central part of Burundi belonging to the Ruvubu River Basin, shows positive anomalies reaching up to 15% (RCP8.5-P2), with exception of RCP8.5-P1, scenario and period for which the median of the CORDEX models simulates practically no change with respect to the reference period.

For the station kag_308 in KRB, Malagarasi river (mal_38), and Lake Tanganyika Basin (tan_81), the median of the hydrological simulations shows a general decrease in annual discharges, in all scenario and periods, however not significative in some cases. The drop in discharge ranges from nearly 0 to − 8.6% (RCP8.5-P1) in kag_308 and tan_81, and from − 2.2% to − 7.1% (RCP4.5-P2) in mal_38.

Regarding the degree of confidence in the simulated sign of change, the increases in discharge count with a higher agreement from the CORDEX models (from 52.6% to 84.2%), especially for RCP8.5-P2 (from 73.6% to 84.2%), while the drops in discharge count with a lower agreement (between 52.6% and 57.9% in most of the cases). For more details, please see table A.3.

Fig. 7b displays the anomalies in the seasonal discharge. As it can be observed, the increments found in the long-term annual discharges in the stations in the KRB are explained by increases taking place along most of the year, with a couple of exceptions found

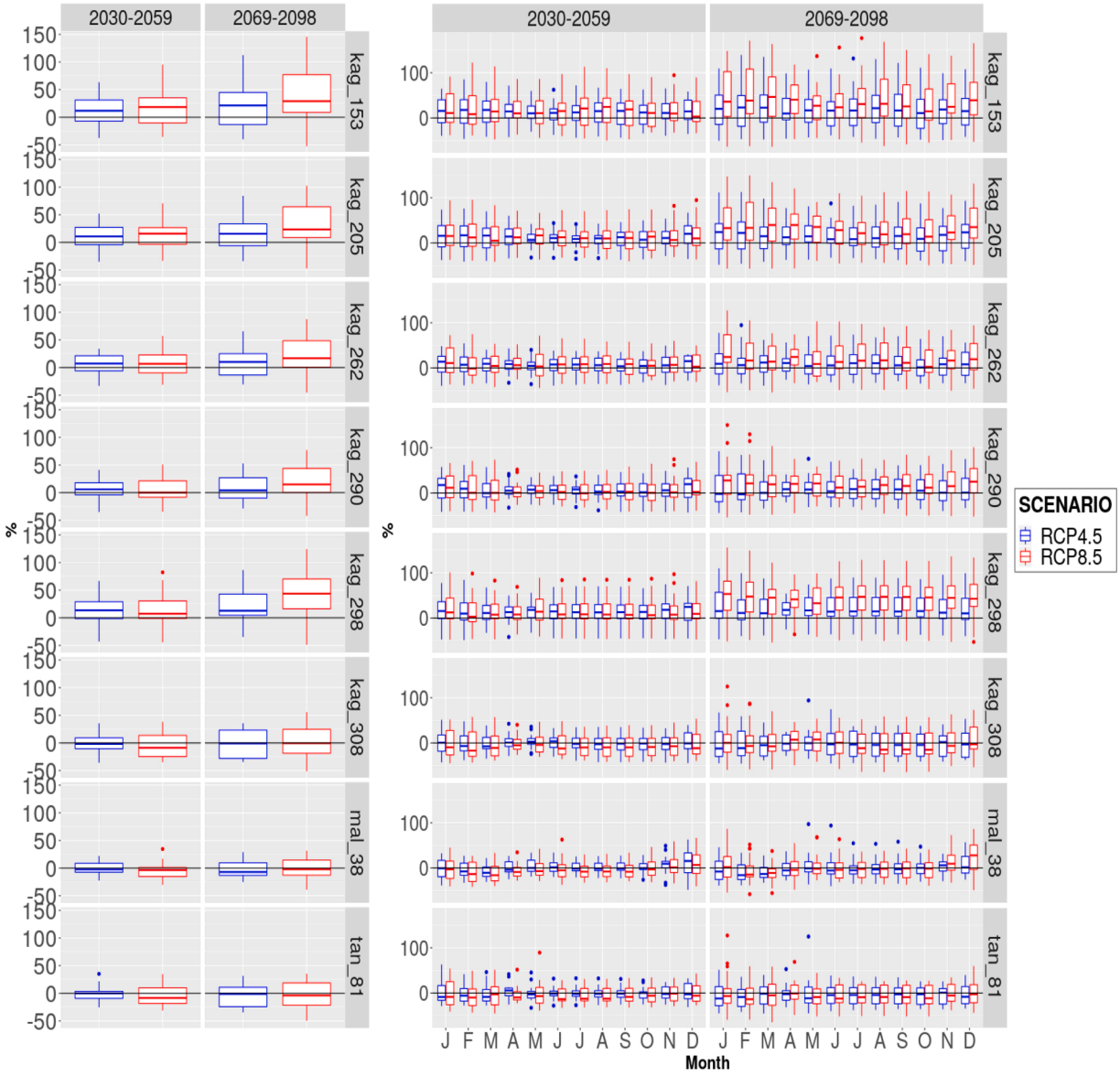

(a) Long-term annual average discharge (b) Long-term monthly average discharge

Fig. 7. Relative anomalies in long-term annual and monthly average discharge for eight gauge stations, under RCPs 4.5 and 8.5, for the future periods P1 (2030–2059) and P2 (2069–2098), in relation to P0 (1970–1999).

in kag_262 and kag_290. In general, it can be seen that such increments are more pronounced during the core months of the short and long rainy seasons (December-January, March-April) and of lower magnitude in the short dry season (February/March) and in October. In the northward stations (kag_153 and kag_262) we also find larger increases over the long dry season (June-September).

The range of the monthly mean anomalies for each station as indicated by the median of the CORDEX models over the scenario-periods are: kag_298 (from 2.8% to 53.1%), kag_153 (approx. from 3.2% to 46.5%), kag_205 (from 5.0% to 39.6%), kag_290 (from −3.1% to 27.7%), and kag_262 (from −1.4% to 24.3%). Thus, we can see some decreases in the stations kag_290 (from January to March, in RCP4.5-P2) and kag_262 (in February, RCP8.5-P1). The anomalies found in RCP8.5-P2 are much higher than the ones found in the other three scenario-periods especially during both rainy seasons and are between approximately 32–51% in kag_298, above 14% in kag_153 and kag_205, 11–27.7% in kag_290, and 2.6–24.3% in kag_262.

On the other hand, the station kag_308 shows a general decrease of discharge across the year, reaching values up to − 16.8% (February, RCP8.5-P1). There are a few exceptions of increase in the rainy months, reaching more significative magnitudes (above 7%) in April and May under the most extreme scenario.

LTB (tan_81) shows negative anomalies throughout the whole year, with only a couple of exceptions indicating no change or an increment of discharge under the moderate emissions scenario. The magnitude of the drop in discharge is higher in January, February,

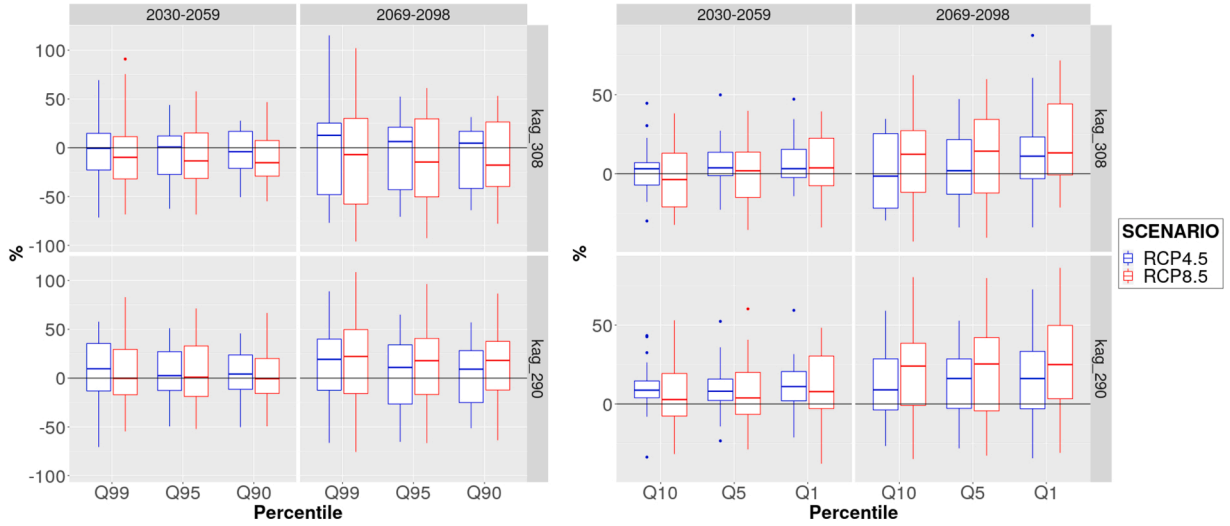

(a) Low flows (Q90, Q95, and Q99) (b) High flows (Q10, Q5, and Q1)

Fig. 8. Relative anomalies in extreme daily flows for two gauge stations (kag_308 and kag_290), under RCPs 4.5 and 8.5, for the future periods P1 (2030–2059) and P2 (2069–2098) in relation to P0 (1970–1999).

and May under both scenarios, and from June to October under RCP8.5, with up to − 13.9% (in February, RCP8.5-P1).

For Malagarasi River, draining the south eastern territory of Burundi (station mal_38), the median of the simulations driven by the CORDEX models indicates a general reduction of monthly mean discharge from January to October (up to −16%), and an increase in November-December (by 1.3–27.9%). The magnitude of decrease would be higher in February and March, in all scenario-periods.

3.3.3. Climate impact on extreme daily discharges

In this section we describe the anomalies for the two stations located within Kagera River Basin, for which we had daily data and calibrated SWIM successfully: kag_308 and kag_290. kag_308 is located upstream of kag_290 (see Fig. 1) and it drains the streamflows from the mountainous area in central-southern Burundi, while kag_290 registers the discharge from the main central part of Burundi, which corresponds to the Ruvubu River Basin.

3.3.3.1. Low flows. The CORDEX ensemble median indicates a decrement in extreme low flows for kag_308, with exception of RCP4.5-P2 that shows increases for the three percentiles under analysis, and RCP4.5-P1 that shows no significant change for Q99 and Q95. The decreases are especially noticeable under RCP8.5, with larger magnitudes found for lower percentiles, up to roughly − 18% for Q90 at the end of the century.

For kag_290 we found a general increment in low flows, however with anomalies very close to 0% for RCP8.5-P1. For the rest of the scenario-periods the median of the simulations show an increase, especially by the end of the century, roughly above 19% and 22% for RCP4.5 and RCP8.5 respectively.

Nonetheless, the range of the magnitudes of change reaches much larger values when considering the models individually, with e.g. anomalies between − 75.7% and 108.6% for kag_290, Q99 and RCP8.5-P2. These and other values regarding the anomalies in low flows can be found in table A.4.

3.3.3.2. High flows. We found robust increases in extreme high discharges for all stations, percentiles, scenarios and periods, except for two cases: Q10 in kag_308, for RCP4.5-P2 and RCP8.5-P1 (see Fig. 8b).

The magnitude of the anomalies is larger for more extreme discharges, except under RCP8.5-P2, where the median of CORDEX models is similar for all percentiles. Hereby, we found median anomalies between − 3.7% and 14.3% in kag_308, and between 2.8% and 25.4% in kag_290 (table A.5 shows detailed information per station, scenario, period, and percentile). Moreover, the minimum and maximum anomalies indicated by specific CORDEX models for kag_308 are − 34.1% and 87.6% (both found in Q1) and for kag_290, − 32.7% (Q5) and 86.25% (Q1), with all extreme values found in RCP8.5-P2.

The confidence of the sign of the anomalies is higher for kag_290 than for kag_308 as well as for RCP4.5-P1 and RCP8.5-P2, compared to the "intermediate" scenario-periods (see table A.5 for more details).

4. Discussion and outlook

4.1. Changes in near-surface mean temperature and precipitation

The CORDEX models show a faster warming over Burundi than the global mean, as it is already known for East Africa (Osima et al.,

2018). The projections analyzed in this study are coherent with the observed increasing trends in annual and seasonal mean temperature found since 1980 in equatorial and southern parts of East Africa, and with the long-term annual mean anomalies projected by an ensemble of Coupled Model Intercomparison Project Phase 5 (CMIP5) models under RCP 8.5 (Niang et al., 2015).

High temperatures have been reported to be the cause of the stratification and consequent decrease in nutrient recharge and primary production dynamics in Lake Tanganyika over the last decades (Tierney et al., 2010). They are also responsible of shorter periods for mosquito's incubation, which increase the transmission of malaria, main cause of mortality in pregnant women and children under five years in Burundi (Baramburiye et al., 2013). Also, poverty in rural areas of Burundi is due, among other factors, to persistent droughts (Baramburiye et al., 2013). Therefore, the severe increase of temperatures found in this study would very likely increase the vulnerability of Burundians and impact the well-being and likelihoods of people.

Regarding precipitation, the opposite signals of change found in the northern and southern territory of Burundi have been also reported in other studies based on CORDEX (Endris et al., 2019; Osima et al., 2018). This pattern, which gets extended over East Africa, has been associated to a stronger and weaker El Niño Southern Oscillation (ENSO)/Indian Ocean Dipole (IOD) related rainfall anomaly over the eastern and southern parts of East Africa respectively (Endris et al., 2019). Such spatial differences have not been detected in studies using only GCMs (Haensler et al., 2013, Nile Basin Initiative, 2018), which supports the use of CORDEX RCMs as a valuable tool to obtain more accurate results in regional studies.

The increment of precipitation in the north of Burundi would need especial attention in areas like Bujumbura, prone to landslides and severe flash-floods (Nkunzimana et al., 2019). In opposition to the general increase of precipitation in the north of Burundi, we also found a decrement of precipitation in February in both, the north and south of the country. This would mean a more severe dry period between both rainy seasons than in the past, fact that would require to take action for adaptation for instance in the provinces of Kirundo and Muyinga, which are located in the north of Burundi and have suffered severe droughts causing people to migrate due to famine (Nkunzimana et al., 2019).

The decrease of precipitation found in the onset months of the rainy season (September-October) in North and South Burundi and in the offset (May) in the south, together with the increase of temperatures projected from May to October, imply a prolongation of the long dry season in Burundi, as it has been likewise reported for East Africa (Wainwright et al., 2019). Such an effect has been already observed in the recent past and farmers have started to adapt by selecting shorter-season crops (Baramburiye et al., 2013).

Moreover, the general decrement of rainfall throughout the whole year in South Burundi, especially from December to February, would compromise the use of water resources and need for water allocation.

4.2. Anomalies in mean river discharge

We found a general increase in the average river discharge in North Burundi and a general decrease in South Burundi that agree with the anomalies found for precipitation in this study as well as by Kim et al. (2021). The later concludes about the rise of seasonal mean and extreme runoff in the Ruvubu River Basin (station kag_290 in this study) as an effect of the intensification of the hydrological cycle, based on the projections from two earth system models in the sixth phase of the Coupled Model Intercomparison Project (CMIP6).

The KRB shows a strong response to the projected rise in precipitation in northern Burundi, with discharges more than folding the reported changes for precipitation in some stations (e.g. annual average change up to 44% in kag_298 in RCP8.5-P2 in response to an increment in precipitation by 20.7% at the most northern cell falling within Burundi). This suggests an increase in extreme precipitation events in KRB, as reported by Kim et al. (2021), that may result in an increment of the runoff due to a reduction of the infiltration of precipitation into the soils. Moreover, higher temperatures would have an effect on the condition of the soils, inducing higher volume of surface runoff from precipitation.

On the other side, our results indicate water stress in the stations draining the southern half of Burundi, with some exceptions in the south-center (kag_308) and south-east (mal_38) of Burundi in the long and short rainy seasons respectively. Here, the magnitudes of change in discharge keep a direct relation with the changes in precipitation, with for instance a maximum decrease of − 13.9% in tan_81, in response to a drop in precipitation of − 13.4%.

Moreover, discharge simulations based on single CORDEX models indicate higher magnitudes of change than the multi-model median. Therefore, such ranges of change should be considered when planning the management of water resources and adaptation strategies designed to combat climate change.

Other factors, like the high population density and high growth rate, should be also taken into account since these may outweigh the potential higher water availability in Burundi in the long-term.

Due to the expected increase in food demand and the inter-annual variability of river discharge, studies about the construction of weirs or small dams that could support crop irrigation during the onset and offset of the rainy season or in case of rainfall failure, should be conducted. In addition, in order to prevent possible upstream-downstream conflicts and to preserve the health of ecosystems in terms of structure and functioning, the potential impacts should be previously explored.

4.3. Anomalies in extreme river discharge

Our simulations show substantial increases in extreme high flows in two stations within KRB: kag_308, located in the southern half of Burundi and registering flows from the Burundian montaneous area (except for Q10), and kag_290, which registers the flows of the Ruvubu River Basin and is located downstream of kag_308. For the extreme low flows, the CORDEX models indicate a robust increase in kag_290, more significant in the far future, and different signs of change in kag_308: an increase in RCP4.5-P2 and a decrease under RCP8.5.

Burundi has been prone to deadly river floods and landslides in the past, especially in the capital city of Bujumbura and its rural surroundings. Examples are the 2006, 2014, and 2016/17 events (EM-DAT, 2018; Nkunzimana et al., 2019), where hundreds of people were affected and many lives were lost. The increase found in extreme high flows within Ruvubu Basin agree with the results of Kim et al. (2021) and implies a higher risk of (flash-)floods and landslides in the main part of Burundi in the future (EM-DAT, 2018). Such results could also involve Bujumbura city and "Bujumbura rural" provinces, however due to the lack of daily discharge data, we could not explore the extremes in discharge in the northern region of LTB. In this regard, Thiery et al. (2016) found that Lake Victoria and Lake Tanganyika are projected to be a hotspot of future extreme precipitation intensification over night, which suggests that our results on extreme high flows could be extended to Bujumbura region.

4.4. Uncertainties and limitations

In order to reduce the error of the CORDEX data and the associated uncertainties due to the propagation of such error along the modeling chain in the current study, we adjusted the bias of the models based on WFD-ERA40. However, the application of the parametrization done with the ISIMIP-BA method, based on the projections in the reference period, to the future projections imply some uncertainties that could play a role in the associated impacts.

Following, the SWIM model was calibrated at the daily and monthly time steps for different stations based on WFD-ERA40. However, we could not calibrate the discharge for gauge stations draining catchments of small size (e.g. in LTB for other gauge stations than tan_81), probably due to the coarse resolution of WFD-ERA40. Climate data with higher resolution would help to better represent the climate in regions with such a complex topography like Burundi, and therefore to obtain more accurate results. However, when performing this study other datasets did not offer data prior to 1979, while WFD-ERA40 data covered the full period required for the calibration and validation of SWIM according to the timeframe of the observations (1970–1999).

Regarding the resolution of the RCMs used in this study, the CORDEX provides nowadays climate data at 0.22 degree resolution, however only for a few models and random RCPs. This is a common problem that could be solved through the fulfillment of the models matrix (Nikulin et al., 2018), which would allow the application of climate projections with higher resolution for climate impact assessments and thus, to obtain more accurate results.

Another source of uncertainty in the results of this study could be the length and quality of the time series used for the calibration of SWIM. The acquisition of discharge data for hydrological studies in African countries is a common problem. In the case of Burundi a civil war took place from 1993 to 2005 (Nantulya, 2015). This is probably the reason why most of the provided time series ended in 1993/94. Additionally, we only could obtain daily data for three stations within KRB. Therefore, the calibration of SWIM was constraint to the availability of discharge data.

Besides the data limitation, the quality of the calibration of the hydrological model is another source of uncertainty in climate impact studies. Nonetheless they have been shown to contribute the least to the uncertainty of projected changes in mean and high flows in several studies (Vetter et al., 2017). In this respect, the SWIM represented properly the flow dynamics, however it did not capture properly all the peaks and base flows existing in the observations. Therefore, the results on streamflows should be treated with caution for the stations and quantiles presenting a large bias in comparison to observed data (e.g. Q99 in kag_308).

Likewise, we acknowledge existing uncertainties in the sign of change projected by the different models, with results becoming more spread towards RCP8.5 and at the end of the 21st century. However, on the other side we have also found a robust consensus from the CORDEX models on the sign of the projected changes for the hydro-climatic variables here explored.

To summarize, despite the uncertainties inherent to the modeling chain, we have shown our results to be coherent with the observed trends and future projections reported in the literature, which show the robustness of the methods and conclusions of this study.

5. Conclusion

People highly dependent on weather patterns to make their living are more vulnerable to the effects from anthropogenic climate change and are in urgent need to cope with the outcome. Yet, the information derived from impact studies is not always available or is less detailed than required. Identifying the potential impacts of climate change is important to implement adaptation actions addressed to reduce adverse consequences.

In this study, we have contributed to filling the gap about the potential hydro-climatic changes to be expected in the future over Burundi, by using a set of the state-of-the-art bias-adjusted CORDEX RCMs and the eco-hydrological model SWIM under two climate scenarios and for two future periods in the 21st century.

A warmer climate, decreasing precipitation at the offset of the rainy season in North Burundi and along most of the year in South Burundi have been projected by the CORDEX climate models for Burundi's future. Such changes pose a high risk to the agricultural production, on which 90% of the population depends. The history has shown that famine, malnutrition, mortality, and related migration among others, are direct consequences of such climate events.

On the other side, increasing precipitation has been projected in North Burundi throughout most of the year and in some exceptional months for some scenario-periods in South Burundi. Soil water conservation techniques and rainfall storage could be used to overcome some of the negative consequences from a warmer future climate; nonetheless it should be kept in mind that under a high-emission scenario, difficulties to adapt will increase dramatically.

An increase in mean and extreme streamflow has been found in the northern and central part of Burundi (Ruvubu basin), while in the south a reduction of discharge would very likely take place along the year, with exception of an increment in some rainy months. These changes call urgently for an effective management of water resources, which may help to mitigate harmful effects of climate

warming, while promoting livelihoods and human development in Burundi. In the south, a better management could help to benefit from the rainfall fallen during the rainy season and balance the reduction of discharge during the rest of the year.

Despite the inherent uncertainties of this study, we have shown that the future anomalies found in the hydro-meteorological indicators analyzed are robust and coherent, between them and with other scientific work. Hence, our results are useful for policy-makers in the water and related sectors, such as agriculture or energy. The uncertainties should be treated carefully, as should other socioeconomic factors such as population growth or land use changes be taken under consideration when planning water resources management and climate change adaptation.

Declaration of Competing Interest

The authors declare that they have no known competing financial interests or personal relationships that could have appeared to influence the work reported in this paper.

Acknowledgments

This work was partially supported by the Deutsche Gesellschaft für Internationale Zusammenarbeit (GIZ) GmbH, Germany [grant number 81167577]. We would like to deeply thank Dr. Marisa Arce for helping to improve this manuscript.

Conflict of interest

The authors declare no conflict of interest.

A. Appendix

A.1. Observed data

See: Table A.1.

Table A.1
Percentage of missing data for observed precipitation, minimum, and maximum temperatures in 18 stations in Burundi. In red, the percentages above 50%. The second table shows the code, name, coordinates, altitude, annual precipitation, minimum, maximum, and mean temperature, for each station.

Missing data (%)	10011	10030	10044	10046	10061	10079	10112	10116	10127
Prec	1.01	12.83	0.33	0.45	13.17	1.70	14.32	14.87	0.84
Tmin	2.53	14.17	17.57	52.70	26.59	15.20	17.82	7.78	1.71
Tmax	3.12	15.41	17.57	52.09	18.09	15.69	2.04	17.82	7.78

Missing data (%)	10143	10164	10052	10095	10098	10142	10161	10166
Prec	16.39	0.05	0.18	33.35	70.90	0.00	1.60	42.20
Tmin	67.13	19.97	13.37	14.99	0.91	44.96	14.27	52.23
Tmax	2.11	38.80	19.75	13.22	14.75	39.77	14.29	71.94

Code	Station	Latitude	Longitude	Altitude (m.)	Annual Prec.	Tmin	Tmax	Tmean
10011	Bujumbura_Aero	− 3.32	29.32	783	782	18.7	29.5	24.1
10030	Cankuzo	− 3.28	30.38	1652	1225	14.4	25.2	19.8
10044	Gisozi	− 3.57	29.68	2097	1454	11	22	16.5
10046	Gitega_aero	− 3.42	29.92	1645	1205	13	25.5	19.25
10052	Imbo_Sems	− 3.18	29.35	820	796	11.6	26.6	19.1
10061	Karuzi	− 3.10	30.17	1600	1110	14.8	27.1	20.95
10075	Kinyinya	− 3.65	30.33	1308	1258	15.7	28	21.8
10079	Kirundo	− 2.58	30.12	1449	1056	15.9	26.9	21.4
10095	Mparambo	− 2.83	29.08	887	940	14.9	25.1	20
10098	Mpota_Tora	− 3.73	29.57	2160	1557	9.7	20.9	15.3
10112	Muriza	− 3.53	30.08	1616	1145	18.7	25.2	21.95
10116	Musasa	− 4.00	30.10	1260	1174	11.6	28.1	19.85
10127	Muyinga	− 2.85	30.35	1756	1118	18.1	20.7	19.4
10142	Nyamuswaga	− 2.88	30.03	1720	1364	17.1	30.3	23.7
10143	Nyanza Lac	− 4.32	29.62	820	1197	9.7	31.3	20.5
10161	Ruvyironza	− 3.82	29.77	1822	1301	11.3	26.9	19.1
10164	Rwegura	− 2.92	29.52	2302	1676	10	24	17
10166	Rweza_vyanda	− 4.10	29.60	1851	1443	12.8	23.1	17.95

A.2. Maps

See: Fig. A.1, Fig. A.2.

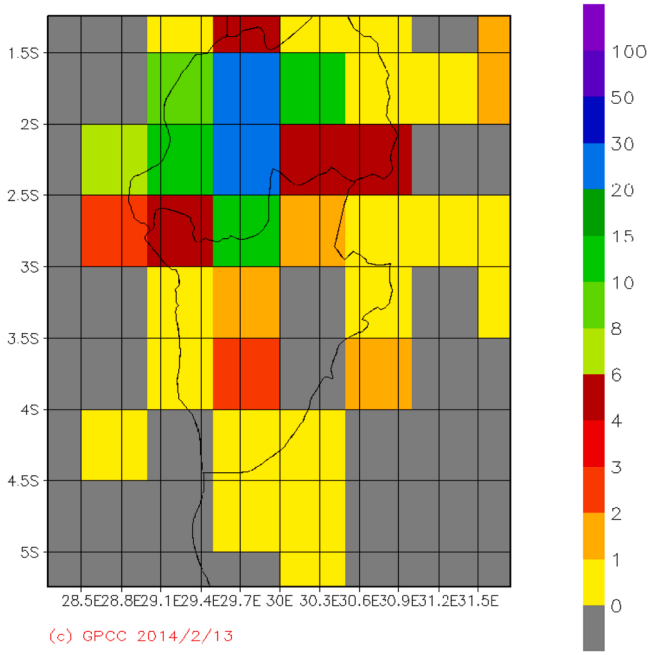

Fig. A.1. Number of stations per grid cell (0.5 degree) used by GPCC Precipitation Climatology Version 2020 (1970–2000)[61].

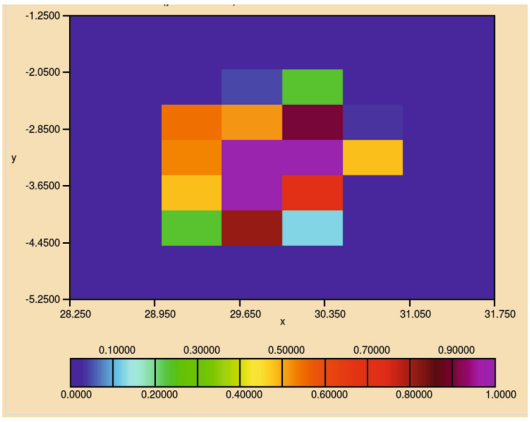

(a) Fractional area coverage mask for Burundi

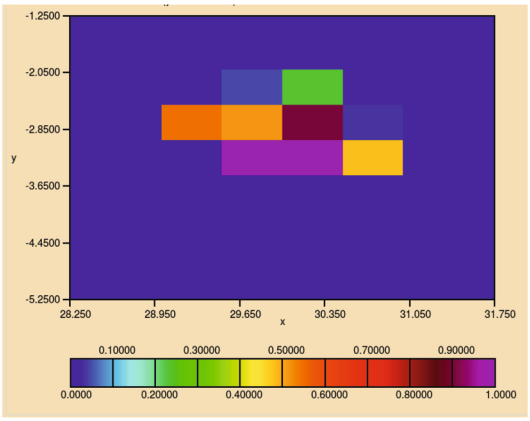

(b) Fractional area coverage mask for North Burundi

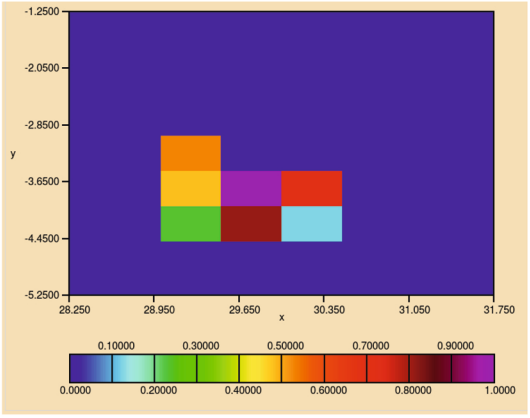

(c) Fractional area coverage mask for South Burundi

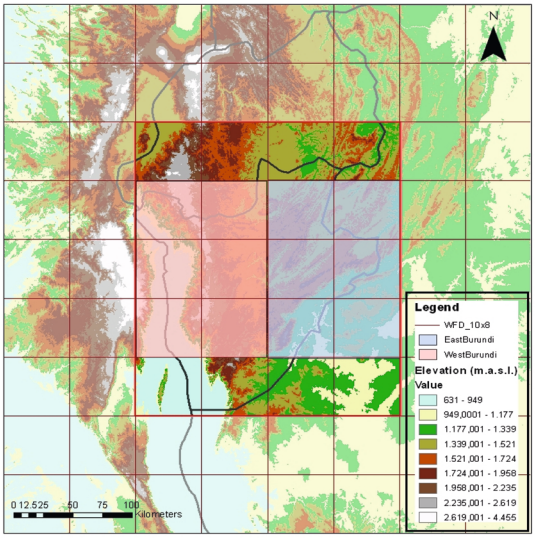

(d) East-West Burundi mask

Fig. A.2. Spatial masks for the averages of climate variables over Burundi.

A.3. Climate

A.3.1. Average climate

See: Fig. A.3, Table A.2.

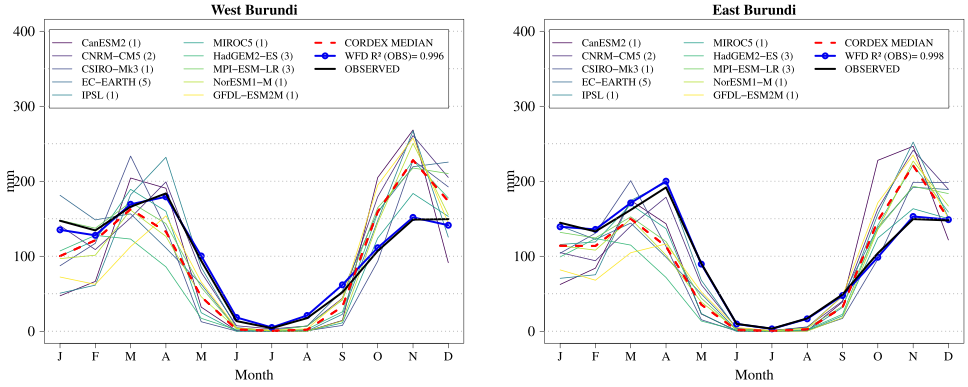

(a) Long-term monthly mean precipitation

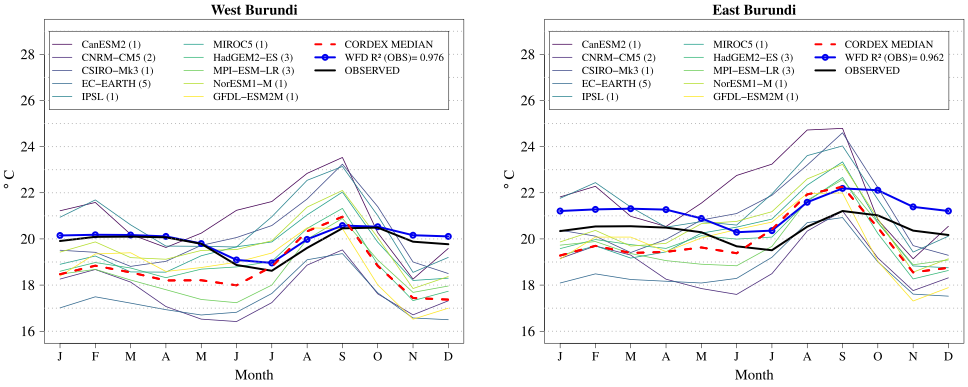

(b) Long-term monthly mean temperature

Fig. A.3. Comparison of seasonal climate in the reference period P0 (1970–1999) in East and West Burundi between WFD-ERA40 and observed data, and original projections from non bias-adjusted CORDEX models for the same period, averaged by GCM. The number of RCMs driven by each GCM is indicated in the legend, between brackets. The CORDEX ensemble median was calculated over 19 GCM-RCM combinations. The correlation between WFD and the observations is given in the legend as WFD R^2 (OBS).

[6] https://kunden.dwd.de/GPCC/Visualizer

Table A.2
Annual average (avg), minimum (min), maximum (max) precipitation and temperature, for each CORDEX GCM (average of the driven RCMs) after bias-adjustment and the CORDEX ensemble median of 19 models for the past (H) over the period (1951–2005) and the future (2006–2099) for both RCPs 4.5 and 8.5. WFD-ERA40 annual average, minimum, and maximum values were calculated over (1951–2001).

Precipitation in North Burundi									
Dataset	Havg	Hmin	Hmax	4.5avg	4.5 min	4.5max	8.5avg	8.5 min	8.5max
CanESM2	1217	878	1591	1186	721	1587	1201	623	1832
CNRM-CM5	1222	830	1465	1197	915	1568	1153	855	1562
CSIRO-Mk3	1197	862	1503	1234	932	1624	1256	839	1655
EC-EARTH	1214	1029	1457	1273	957	1619	1302	910	1725
IPSL	1206	880	1634	1240	780	1699	1272	881	1762
MIROC5	1222	891	1800	1381	999	1909	1419	977	1926
HadGEM2-ES	1160	900	1434	1208	906	1641	1267	860	1636
MPI-ESM-LR	1222	823	1547	1167	810	1503	1151	878	1442
NorESM1-M	1184	948	1504	1315	910	1850	1318	896	1805
GFDL-ESM2M	1176	902	1533	1233	780	1680	1229	774	1669
CORDEX Median	1203	1057	1316	1053	1430	1247	1505	1093	1505
WFD	1237	1026	1539						
Precipitation in South Burundi									
Dataset	Havg	Hmin	Hmax	4.5avg	4.5 min	4.5max	8.5avg	8.5 min	8.5max
CanESM2	1218	887	1555	1081	599	1444	1045	576	1476
CNRM-CM5	1212	886	1489	1169	930	1496	1116	814	1491
CSIRO-Mk3	1203	929	1544	1128	883	1434	1125	750	1476
EC-EARTH	1214	1042	1461	1199	913	1398	1202	910	1491
IPSL	1212	973	1493	1131	750	1515	1117	824	1600
MIROC5	1212	905	1771	1254	896	1608	1267	886	1689
HadGEM2-ES	1168	871	1386	1205	844	1496	1230	970	1688
MPI-ESM-LR	1225	937	1555	1109	833	1390	1067	786	1379
NorESM1-M	1191	930	1521	1217	929	1664	1202	870	1617
GFDL-ESM2M	1199	884	1462	1123	821	1526	1091	798	1496
CORDEX Median	1205	1085	1315	1172	985	1339	1151	971	1327
WFD	1247	985	1525						
Near-surface mean temperature averaged over Burundi									
Dataset	Havg	Hmin	Hmax	4.5avg	4.5 min	4.5max	8.5avg	8.5 min	8.5max
CanESM2	20.3	19.5	21.3	0.4	22.6	20.9	23.8	0.7	23.7
CNRM-CM5	20.4	19.7	21.2	0.3	− 112.7	− 114.5	− 111.4	0.7	− 111.8
CSIRO-Mk3	20.5	19.9	21.2	0.3	22.7	20.7	24.2	1	23.4
EC-EARTH	20.3	19.4	20.9	0.3	21.8	20.6	22.7	0.6	22.6
IPSL	20.4	19.6	21.5	0.4	22.8	21.1	24.2	0.9	23.9
MIROC5	20.5	19.8	21.8	0.4	22.3	20.7	23.7	0.7	23.1
HadGEM2-ES	20.4	19.6	21	0.3	22.6	20.9	24	0.8	23.5
MPI-ESM-LR	20.3	19.5	21.4	0.4	22.1	20.8	23.4	0.7	23.2
NorESM1-M	20.4	19.7	21	0.3	22	20.9	22.9	0.5	22.7
GFDL-ESM2M	20.4	19.4	21.4	0.5	22.4	21.2	23.3	0.6	23.3
CORDEX Median	20.4	19.9	21.1	0.3	22.1	20.9	23.1	0.6	23
WFD	20.3	19.6	21.3	0.4					

A.3.2. Anomalies of long-term annual average temperature

See: Fig. A.4.

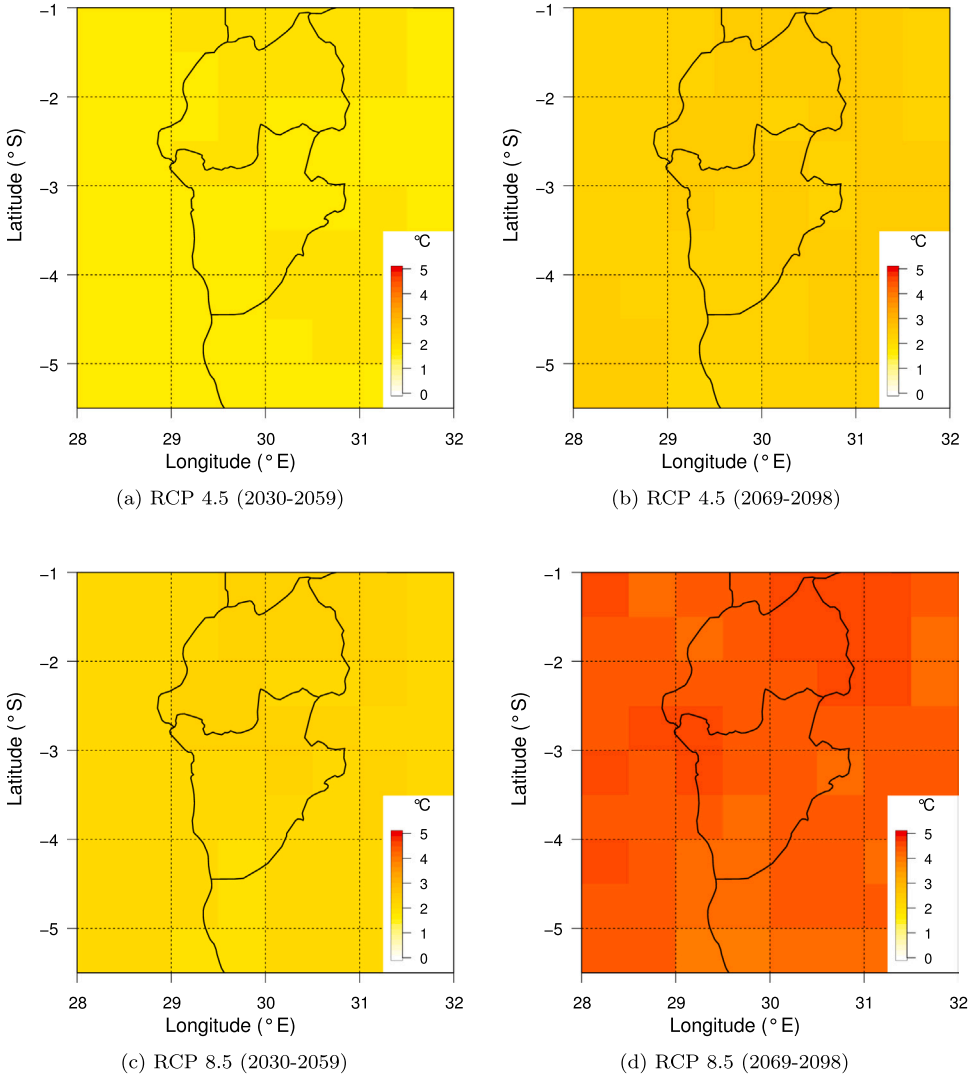

(a) RCP 4.5 (2030-2059) (b) RCP 4.5 (2069-2098)

(c) RCP 8.5 (2030-2059) (d) RCP 8.5 (2069-2098)

Fig. A.4. Spatial distribution of changes in annual mean temperature projected by the median of CORDEX models.

A.4. Hydrological processes

A.4.1. Model evaluation

See: Fig. A.5, Fig. A.6, Fig. A.7, Fig. A.8.

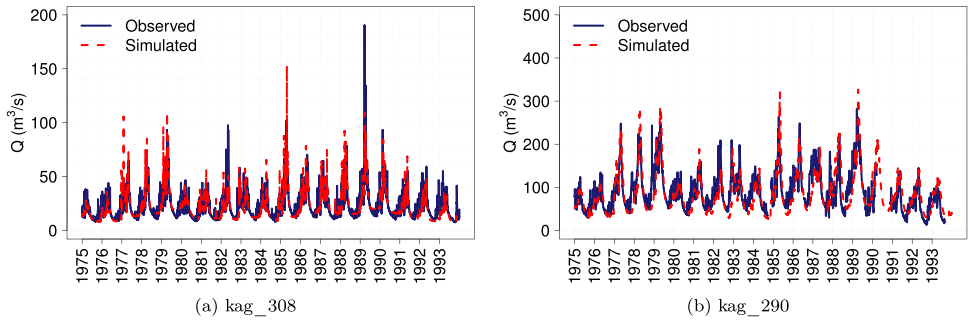

(a) kag_308 (b) kag_290

Fig. A.5. Observed and simulated daily discharge for two stations during the combined calibration and validation period (1975–1993).

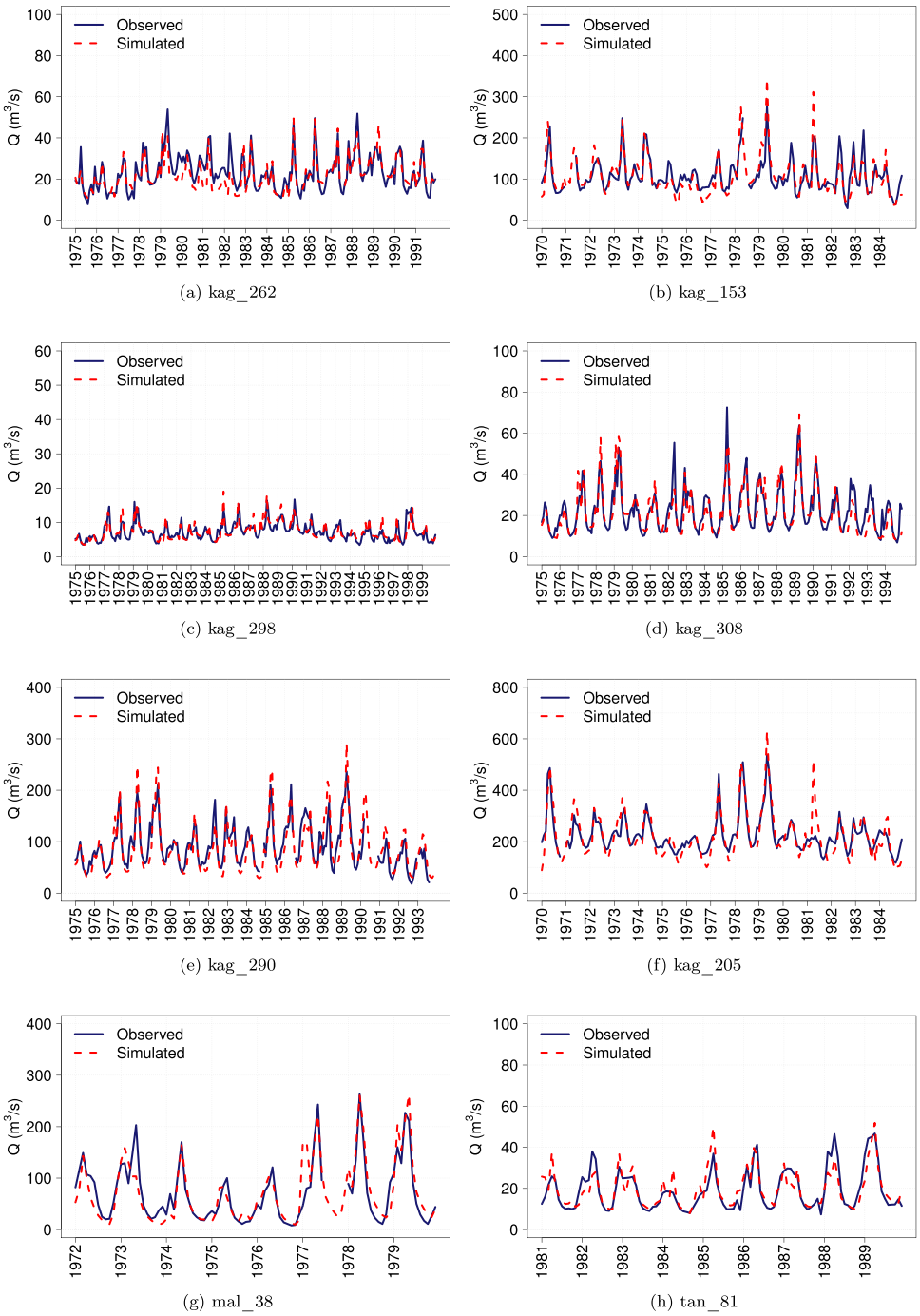

Fig. A.6. Observed and simulated mean monthly discharge for eight stations during the combined calibration and validation periods.

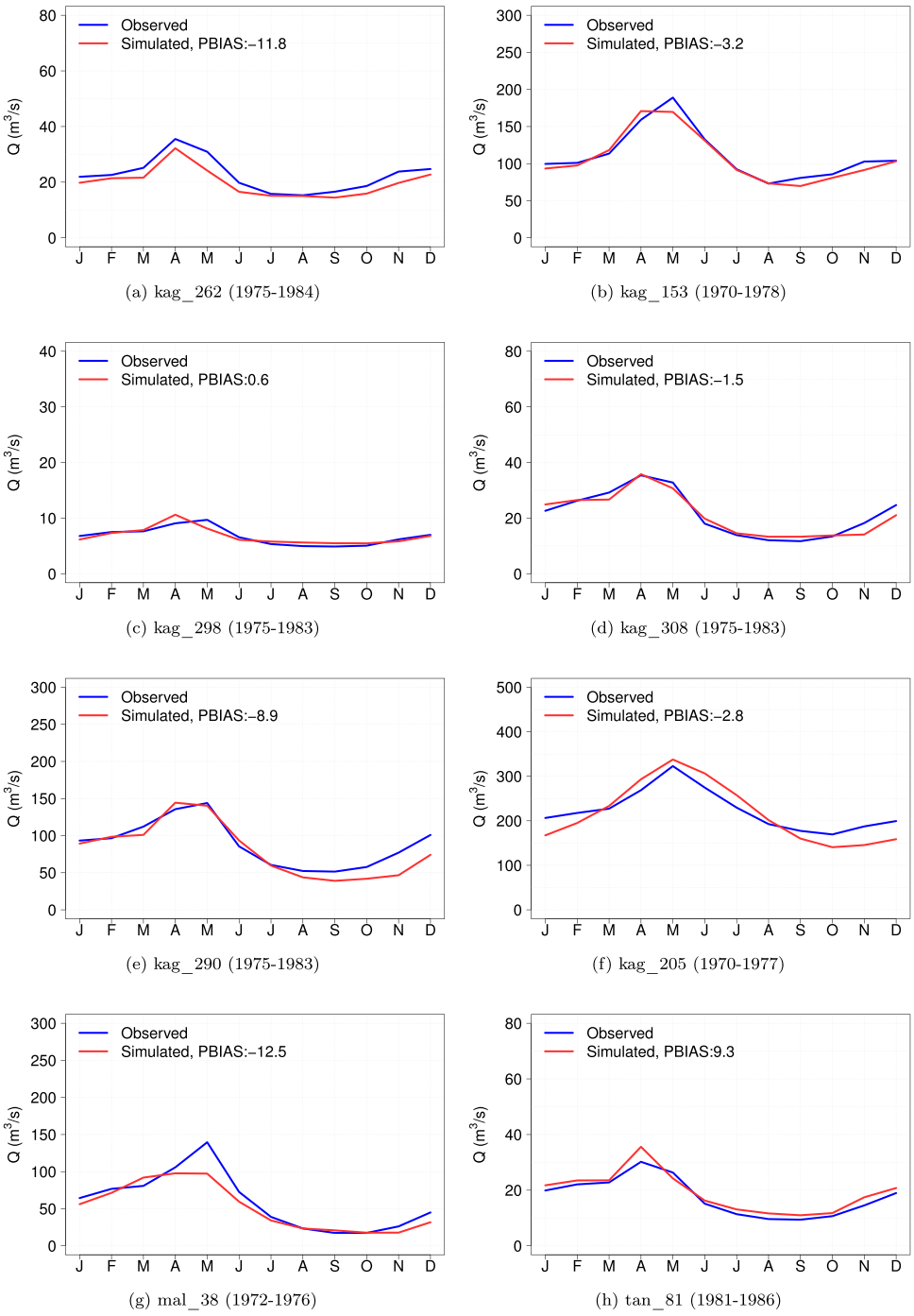

Fig. A.7. Observed and simulated long-term mean monthly discharge for eight stations in the calibration period.

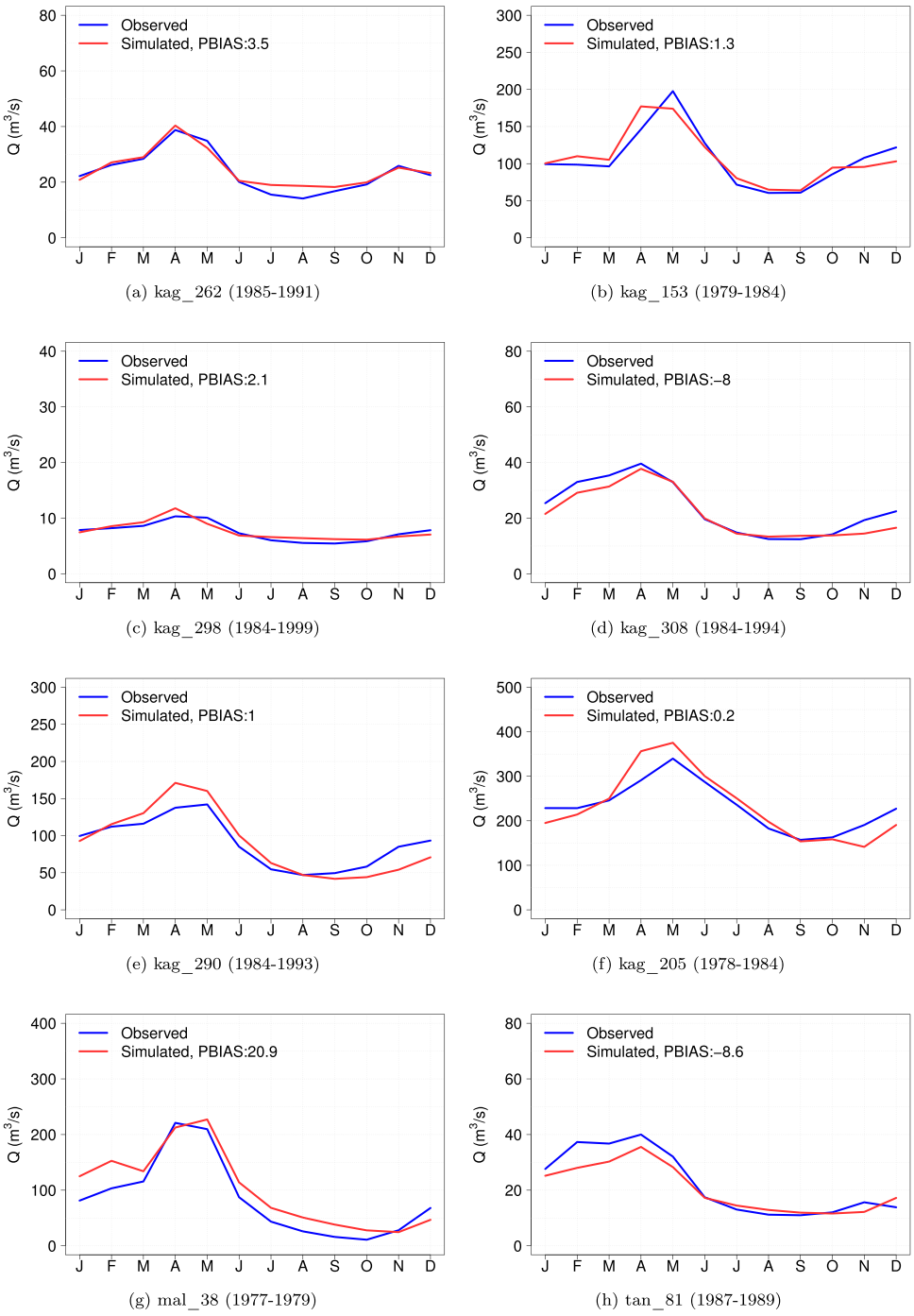

Fig. A.8. Observed and simulated long-term mean monthly discharge for eight stations in the validation period.

A.4.2. Anomalies in long-term annual mean discharge

See: Table A.3.

Table A.3
Statistics applied to the anomalies of the long-term annual mean discharge simulated by SWIM driven by 19 CORDEX models for eight gauge stations under RCPs 4.5 and 8.5, for the periods P1 (2030–2059) and P2 (2069–2098), in relation to P0 (1970–1099): %median (relative mean of the CORDEX anomalies), median (absolute median of the CORDEX anomalies), Interquantile Range (IQR of the rel. anom.), standard deviation (SD of the rel. anom.), minimum and maximum rel. anom. indicated by the models, percentage of models indicating a decrease (%Neg) or an increase (%Pos).

Scenario	Station	%Median	Median	IQR	SD	Min	Max	%Neg	%Pos
RCP4.5-P1	kag_153	11.78	12.71	38.01	28.2	− 37.5	63.4	31.58	68.42
RCP4.5-P1	kag_205	10.81	24.18	31.41	23.44	− 35.07	52.06	31.58	68.42
RCP4.5-P1	kag_262	7.2	1.46	27.27	19.73	− 33.38	33.95	31.58	68.42
RCP4.5-P1	kag_290	5.98	4.71	21.84	18.46	− 35.17	41.1	42.11	57.89
RCP4.5-P1	kag_298	13.54	0.98	30.53	25.23	− 42.89	66.77	31.58	68.42
RCP4.5-P1	kag_308	− 1.67	− 0.34	19.62	17.75	− 35.86	35.56	52.63	47.37
RCP4.5-P1	mal_38	− 2.36	− 2.07	16.01	11.5	− 22.7	22.06	57.89	42.11
RCP4.5-P1	tan_81	− 0.06	− 0.01	12.84	14.9	− 25.58	35.09	52.63	47.37
RCP4.5-P2	kag_153	21.36	24.12	57.88	41.94	− 39.92	112.44	36.84	63.16
RCP4.5-P2	kag_205	15.64	34.97	39.52	33.97	− 34.04	84.26	36.84	63.16
RCP4.5-P2	kag_262	10.06	2.04	38.66	27.42	− 30.63	65.45	42.11	57.89
RCP4.5-P2	kag_290	4.09	3.37	36.78	25.49	− 28.57	53.02	47.37	52.63
RCP4.5-P2	kag_298	12.83	0.92	38.35	33.14	− 34.72	86.47	21.05	78.95
RCP4.5-P2	kag_308	− 0.79	− 0.16	51.25	26	− 34.46	35.72	57.89	42.11
RCP4.5-P2	mal_38	− 7.1	− 5.66	22.69	16.55	− 25.15	28.83	52.63	47.37
RCP4.5-P2	tan_81	− 1.21	− 0.19	35.06	21.1	− 34.62	31.61	57.89	42.11
RCP8.5-P1	kag_153	18.34	18.76	45.39	37.99	− 35.47	95.16	42.11	57.89
RCP8.5-P1	kag_205	16.01	34.34	30.11	31.68	− 33.42	70.75	36.84	63.16
RCP8.5-P1	kag_262	6.77	1.37	32.48	26.03	− 31.04	57.14	47.37	52.63
RCP8.5-P1	kag_290	0.23	0.19	29.58	24.77	− 34.69	51.13	47.37	52.63
RCP8.5-P1	kag_298	7.25	0.54	31.75	33.14	− 44.32	82.26	31.58	68.42
RCP8.5-P1	kag_308	− 8.66	− 1.64	38.34	23.97	− 34.69	38.32	57.89	42.11
RCP8.5-P1	mal_38	− 3.66	− 2.99	16.45	16.62	− 30.26	34.6	68.42	31.58
RCP8.5-P1	tan_81	− 8.62	− 1.34	28.23	19.47	− 31.3	34.64	52.63	47.37
RCP8.5-P2	kag_153	29.01	31.29	68.17	54.84	− 52.6	145.53	21.05	78.95
RCP8.5-P2	kag_205	23.47	52.48	55.68	44.47	− 47.31	102.75	21.05	78.95
RCP8.5-P2	kag_262	16.6	3.5	47.92	36.01	− 45.23	87.52	26.32	73.68
RCP8.5-P2	kag_290	14.9	12.28	43.31	33.84	− 41.81	77.22	26.32	73.68
RCP8.5-P2	kag_298	43.75	3.11	54.05	45.33	− 48.71	124.51	15.79	84.21
RCP8.5-P2	kag_308	− 0.42	− 0.08	43.38	32.83	− 51.48	55.79	52.63	47.37
RCP8.5-P2	mal_38	− 2.18	− 1.78	27.32	20.97	− 39.01	31.47	52.63	47.37
RCP8.5-P2	tan_81	− 3.95	− 0.61	40.28	26.4	− 49.91	35.34	57.89	42.11

A.4.3. Anomalies in daily extreme discharges

See: Table A.4, Table A.5.

Table A.4
Statistics applied to the anomalies of the low flows (percentiles Q90, Q95, and Q99) simulated by SWIM driven by 19 CORDEX models for eight gauge stations under RCPs 4.5 and 8.5, for the periods P1 (2030–2059) and P2 (2069–2098) in relation to P0 (1970–1099): %median (relative mean of the CORDEX anomalies), median (absolute median of the CORDEX anomalies), Interquantile Range (IQR of the rel. anom.), standard deviation (SD of the rel. anom.), minimum and maximum rel. anom. indicated by the models, percentage of models indicating a decrease (%Neg) or an increase (%Pos).

Station	Scenario	Pctl	%Median	Median	IQR	SD	Min	Max	%Neg	%Pos
kag_290	RCP4.5-P1	Q90	4.1	1.24	35.23	24.6	− 50.26	45.77	36.84	63.16
kag_290	RCP4.5-P2	Q90	9.11	3.34	53.3	33.21	− 51.49	57.03	42.11	57.89
kag_290	RCP8.5-P1	Q90	− 0.6	− 0.2	35.86	32.58	− 49.42	66.7	52.63	47.37
kag_290	RCP8.5-P2	Q90	18.09	5.41	49.83	42.63	− 63.67	86.61	31.58	68.42
kag_290	RCP4.5-P1	Q95	2.44	0.79	39.83	28.4	− 49.51	51.1	42.11	57.89
kag_290	RCP4.5-P2	Q95	11	3.57	60.61	37.47	− 65.32	65.03	42.11	57.89
kag_290	RCP8.5-P1	Q95	0.9	0.25	51.72	35.01	− 52.22	71.39	47.37	52.63
kag_290	RCP8.5-P2	Q95	17.83	4.52	57.34	46.88	− 66.63	96.4	31.58	68.42
kag_290	RCP4.5-P1	Q99	9.57	2.49	48.65	33.19	− 70.67	57.81	36.84	63.16
kag_290	RCP4.5-P2	Q99	19.17	3.71	52.43	40.58	− 66.37	88.95	42.11	57.89
kag_290	RCP8.5-P1	Q99	− 0.25	− 0.04	46.49	40.92	− 54.73	82.89	52.63	47.37
kag_290	RCP8.5-P2	Q99	22.13	4.56	65.69	55.8	− 75.72	108.63	31.58	68.42
kag_308	RCP4.5-P1	Q90	− 4.04	− 0.42	37.85	23.71	− 50.72	27.7	52.63	47.37
kag_308	RCP4.5-P2	Q90	4.72	0.4	58.51	34.2	− 64.03	31.37	47.37	52.63

(continued on next page)

Table A.4 (*continued*)

Station	Scenario	Pctl	%Median	Median	IQR	SD	Min	Max	%Neg	%Pos
kag_308	RCP8.5-P1	Q90	− 15.38	− 1.14	36.55	30.9	− 54.86	46.75	63.16	36.84
kag_308	RCP8.5-P2	Q90	− 17.78	− 1.62	66.08	43.07	− 77.84	53.12	63.16	36.84
kag_308	RCP4.5-P1	Q95	0.73	0.06	39.32	27.74	− 62.55	43.82	42.11	57.89
kag_308	RCP4.5-P2	Q95	6.39	0.46	64.11	39.69	− 70.67	52.37	47.37	52.63
kag_308	RCP8.5-P1	Q95	− 13.52	− 0.88	46.72	36.34	− 68.37	57.78	57.89	42.11
kag_308	RCP8.5-P2	Q95	− 14.65	− 0.87	80.01	49.78	− 92.71	61.16	57.89	42.11
kag_308	RCP4.5-P1	Q99	− 0.52	− 0.02	37.56	34.65	− 71.43	69.3	52.63	47.37
kag_308	RCP4.5-P2	Q99	12.74	0.55	73.33	52.98	− 76.91	115.18	42.11	57.89
kag_308	RCP8.5-P1	Q99	− 9.82	− 0.33	43.36	45.24	− 68.31	90.91	57.89	42.11
kag_308	RCP8.5-P2	Q99	− 7	− 0.43	87.81	60.12	− 96.08	102.06	52.63	47.37

Table A.5
Idem as A.4 for high flows (percentiles Q1, Q5, and Q10).

Station	Scenario	Pctl	%Median	Median	IQR	SD	Min	Max	%Neg	%Pos
kag_290	RCP4.5-P1	Q1	11.03	25.84	18.57	17.37	− 21.2	59.33	15.79	84.21
kag_290	RCP4.5-P2	Q1	16.17	37.84	36.39	28.26	− 34.42	72.67	36.84	63.16
kag_290	RCP8.5-P1	Q1	7.83	18.97	33.23	25.37	− 37.85	48.28	31.58	68.42
kag_290	RCP8.5-P2	Q1	24.98	64.94	46.45	31.4	− 30.96	86.25	21.05	78.95
kag_290	RCP4.5-P1	Q5	8.11	15.52	13.59	18.37	− 23.35	52.35	21.05	78.95
kag_290	RCP4.5-P2	Q5	16.18	25.98	31.34	21.5	− 28.08	52.77	31.58	68.42
kag_290	RCP8.5-P1	Q5	3.86	6.52	26.63	23.15	− 28.77	60.26	47.37	52.63
kag_290	RCP8.5-P2	Q5	25.35	51.45	46.39	31.19	− 32.71	79.8	31.58	68.42
kag_290	RCP4.5-P1	Q10	8.75	12.8	10.64	17.82	− 33.68	43.36	15.79	84.21
kag_290	RCP4.5-P2	Q10	8.96	13.49	32.33	23.61	− 26.65	59.04	31.58	68.42
kag_290	RCP8.5-P1	Q10	2.83	4.21	27.01	22.8	− 31.71	53.02	42.11	57.89
kag_290	RCP8.5-P2	Q10	24.04	36.94	39.36	32.48	− 34.89	80.42	26.32	73.68
kag_308	RCP4.5-P1	Q1	3.2	1.55	17.88	16.06	− 14.23	47.21	31.58	68.42
kag_308	RCP4.5-P2	Q1	11.12	6.48	26.48	27.54	− 34	87.61	31.58	68.42
kag_308	RCP8.5-P1	Q1	3.67	2.02	30.13	20.85	− 34.08	39.46	42.11	57.89
kag_308	RCP8.5-P2	Q1	13.19	6.44	45.01	28.78	− 21.45	71.73	31.58	68.42
kag_308	RCP4.5-P1	Q5	3.69	1.09	14.88	16.89	− 22.87	49.91	31.58	68.42
kag_308	RCP4.5-P2	Q5	1.91	− 0.51	34.57	22.02	− 34.05	47.3	47.37	52.63
kag_308	RCP8.5-P1	Q5	1.86	− 1.24	28.71	20.68	− 35.63	39.84	42.11	57.89
kag_308	RCP8.5-P2	Q5	14.26	3.92	46.62	29.05	− 40.58	59.89	36.84	63.16
kag_308	RCP4.5-P1	Q10	3.13	1.41	14.1	16.87	− 30	44.58	36.84	63.16
kag_308	RCP4.5-P2	Q10	− 1.6	0.74	47.2	23.09	− 29.62	34.68	52.63	47.37
kag_308	RCP8.5-P1	Q10	− 3.73	0.72	34.09	21.82	− 32.43	38.21	57.89	42.11
kag_308	RCP8.5-P2	Q10	12.33	5.52	39.08	29.68	− 42.97	62.38	47.37	52.63

References

Arnold, J.G., Allen, P.M., Bernhardt, G., 1993. A comprehensive surface-groundwater flow model. J. Hydrol. 142 (1–4), 47–69. https://doi.org/10.1016/0022-1694(93)90004-S.

Baramburiye, J., Kyotalimye, M., Thomas, T.S., Waithaka, M., 2013. East African agriculture and climate change: a comprehensive analysis - Burundi. Int. Food Policy Res. Inst.

Di Baldassarre, G., Elshamy, M., van Griensven, A., Soliman, E., Kigobe, M., Ndomba, P., Mutemi, J., Mutua, F., Moges, S., Xuan, Y., ri Solomatine, D., Uhlenbrook, S., 2011. Future hydrology and climate in the River Nile basin: a review. Hydrol. Sci. J. - J. Des. Sci. Hydrol. 56 (2), 199–211. https://doi.org/10.1080/02626667.2011.557378.

Dosio, A., Jones, R.G., Jack, C., Lennard, C., Nikulin, G., Hewitson, B., 2019. What can we know about future precipitation in Africa? Robustness, significance and added value of projections from a large ensemble of regional climate models. Clim. Dyn. 53, 5833–5858. https://doi.org/10.1007/s00382-019-04900-3.

EM-DAT: The Emergency Events Database - Universite catholique de Louvain (UCL) - CRED, D. Guha-Sapir - www.emdat.be, Brussels, Belgium. Last accessed 15th February, 2018.

Endris, H.S., Omondi, P., Jain, S., Lennard, C., Hewitson, B., Chang'a, L., Awange, J.L., Dosio, A., Ketiem, P., Nikulin, G., Panitz, H.J., Büchner, M., Stordal, F., Tazalika, L., 2013. Assessment of the performance of CORDEX regional climate models in simulating East African rainfall. J. Clim. 26 (21), 8453–8475. https://doi.org/10.1175/JCLI-D-12-00708.1.

Endris, H.S., Lennard, C., Hewitson, B., Dosio, A., Nikulin, G., Panitz, H.J., 2016. Teleconnection responses in multi-GCM driven CORDEX RCMs over Eastern Africa. Clim. Dyn. 46 (9–10), 2821–2846. https://doi.org/10.1007/s00382-015-2734-7.

Endris, H.S., Lennard, C., Hewitson, B., Dosio, A., Nikulin, G., Artan, G.A., 2019. Future changes in rainfall associated with ENSO, IOD and changes in the mean state over Eastern Africa. Clim. Dyn. 52 (3–4), 2029–2053. https://doi.org/10.1007/s00382-018-4239-7.

Fischer, G., F. Nachtergaele, S. Prieler, H.T. van Velthuizen, L. Verelst, D. Wiberg, 2008.Global Agro-ecological Zones Assessment for Agriculture (GAEZ 2008).IIASA, Laxenburg, Austria and FAO, Rome, Italy.

FAO-UN, 2016, Burundi. Situation Report - December 2016.http://www.fao.org/3/a-bs128e.pdf.Last accessed June, 2018.

FAO-UN, 2020, FAO in emergencies. Burundi.http://www.fao.org/emergencies/countries/detail/en/c/161508/.Last accessed May, 2020.

Giorgi, F., Jones, C., Asrar, G., 2009. Addressing climate information needs at the regional level: the CORDEX framework. Organ. (WMO) Bull. 58 (July), 175–183.

Global Water Partnership, 2011, Page last edited: 5/25/2011.⟨https://www.gwp.org/en/WACDEP/IMPLEMENTATION/Where/Burundi⟩.Last accessed January, 2019.

Haensler, A., Saeed, F., Jacob, D., 2013. Assessing the robustness of projected precipitation changes over central Africa on the basis of a multitude of global and regional climate projections. Clim. Change 121 (2), 349–363. https://doi.org/10.1007/s10584-013-0863-8.

ICPAC. Kenya and SEI Oxford Office, 2009, DFID Economic impacts of climate change: Kenya, Rwanda, Burundi. Climate report Burundi.⟨https://www.weadapt.org/sites/weadapt.org/files/legacy-new/knowledge-base/files/4e25a570c28318C-Kenya-East-Africa-climate-science-and-impacts.pdf⟩.
IFRC, International Federation of Red Cross and Red Crescent Societies. (April, 2019). Baseline Survey Report. Strengthening disaster risk reduction capacity for communities hosting IDPs and returnees. https://reliefweb.int/report/burundi/baseline-survey-report-strengthening-disaster-risk-reduction-capacity-communities. Last accessed December, 2020.
IPCC, 2014: Climate Change 2014: Impacts, Adaptation, and Vulnerability. Part B: Regional Aspects. Contribution of Working Group II to the Fifth Assessment Report of the Intergovernmental Panel on Climate Change [Barros, V.R., C.B. Field, D.J. Dokken, M.D. Mastrandrea, K. J. Mach, T.E. Bilir, M. Chatterjee, K.L. Ebi, Y.O. Estrada, R.C. Genova, B. Girma, E.S. Kissel, A.N. Levy, S. MacCracken, P.R. Mastrandrea, and L.L. White, (eds.)]. Cambridge University Press, Cambridge, United Kingdom and New York, NY, USA, 688.
IOM, 2019, Burundi - Internal Displacement Dashboard (December 2019).https://displacement.iom.int/node/7596.Last accessed May, 2020.
Jarvis, A., Reuter, H.I., Nelson, A., Guevara, E., 2008, Hole-filled seamless SRTM data V4, International Centre for Tropical Agriculture (CIAT), available from http://srtm.csi.cgiar.org.
Kim, J.B., Habimana, J. de D., Kim, S.H., Bae, D.H., 2021. Assessment of climate change impacts on the hydroclimatic response in burundi based on cmip6 esms. Sustainability 2021 13 (21), 12037. https://doi.org/10.3390/su132112037.
Kalensky, Z.D., 1998. AFRICOVER Land Cover Database and Map of Africa. Can. J. Remote Sens. 24 (3), 292–297. https://doi.org/10.1080/07038992.1998.10855250.
Kamungi, P., Oketch, J.S., Huggins, C., 2005. Land Access and the Return and Resettlement of? IDPs and Refugees in Burundi. Ground : Land Rights, Confl. Peace Sub-Sahar. Afr. 117–194.
Krysanova, V., Meiner, A., Roosaare, J., Vasilyev, A., 1989. Simulation modelling of the coastal waters pollution from agricultural watersched. Ecol. Model. 49, 7–29.
Krysanova, V., Müller-Wohlfeil, D., Becker, A., 1998. Development and test of a spatially distributed hydrological/water quality model for mesoscale watersheds. Ecol. Model. 261–289.
Krysanova, V., Hattermann, F., Huang, S., Hesse, C., Vetter, T., Liersch, S., Koch, H., Kundzewicz, Zbigniew, W., 2015. Modelling climate and land use change impacts with SWIM: lessons learnt from multiple applications. Hydrol. Sci. J. 2015 (60), 606–635. https://doi.org/10.1080/02626667.2014.925560.
Lange, S.: Trend-preserving bias adjustment and statistical downscaling with ISIMIP3BASD (v1.0), Geosci. Model Dev., 12, 2019: 3055–3070, 10.5194/gmd-12–3055-2019.
Mann, H.B., 1945. Non-parametric tests against trend. Econometrica 13, 245–259. https://doi.org/10.2307/1907187.
Meinshausen, M., Smith, S.J., Calvin, K., Daniel, J.S., Kainuma, M.L.T., Lamarque, J., Matsumoto, K., Montzka, S.A., Raper, S.C.B., Riahi, K., Thomson, A., Velders, G. J.M., van Vuuren, D.P.P., 2011. The RCP greenhouse gas concentrations and their extensions from 1765 to 2300. Clim. Change 109 (1), 213–241. https://doi.org/10.1007/s10584-011-0156-z.
Moriasi, D.N., Arnold, J.G., Van Liew, M.W., Bingner, R.L., Harmel, R.D., Veith, T.L., 2007. Model evaluation guidelines for systematic quantification of accuracy in watershed simulations. Trans. ASABE 50, 885–900. https://doi.org/10.13031/2013.23153.
Moss, R.H., Edmonds, J.A., Hibbard, K.A., Manning, M.R., Rose, S.K., Van Vuuren, D.P., Carter, T.R., Emori, S., Kainuma, M., Kram, T., Meehl, G.A., Mitchell, J.F.B., Nakicenovic, N., Riahi, K., Smith, S.J., Stouffer, R.J., Thomson, A.M., Weyant, J.P., Wilbanks, T.J., 2010. The next generation of scenarios for climate change research and assessment. Nature 463 (7282), 747–756. https://doi.org/10.1038/nature08823.
Nantulya, P., 2015, 08–05, Burundi: Why the Arusha Accords are Central. Africa Center for Strategic Studies.⟨https://africacenter.org/spotlight/burundi-why-the-arusha-accords-are-central⟩.Last accessed, April 2022.
Nash, J.E., Sutcliffe, J.V., 1970. River flow forecasting through conceptual models part I - A discussion of principles. J. Hydrol. 10 (3), 282–290. https://doi.org/10.1016/0022-1694(70)90255-6.
NAPA: National Adaptation Plan of Action to climate change, 2007, Ministry for Land Management, Tourism and Environment, Republic of Burundi.⟨https://www.adaptation-undp.org/sites/default/files/downloads/burundi_napa.pdf⟩.
Niang, I., Ruppel, O. C., Abdrabo, M. A., Essel, A., Lennard, C., Padgham, J., & Urquhart, P., 2015, Africa. Climate Change 2014: Impacts, Adaptation and Vulnerability: Part B: Regional Aspects: Working Group II Contribution to the Fifth Assessment Report of the Intergovernmental Panel on Climate Change, 1199–1266.10.1017/CBO9781107415386.002.
Nikulin, G., Jones, C., Giorgi, F., Asrar, G., Büchner, M., Cerezo-Mota, R., Christensen, O.B., Déqué, M., Fernandez, J., Hänsler, A., van Meijgaard, E., Samuelsson, P., Sylla, M.B., Sushama, L., 2012. Precipitation climatology in an ensemble of CORDEX-Africa regional climate simulations. J. Clim. 25 (18), 6057–6078. https://doi.org/10.1175/JCLI-D-11-00375.1.
Nikulin, G., Lennard, C., Dosio, A., Kjellström, E., Chen, Y., Hansler, A., Kupiainen, M., Laprise, R., Mariotti, L., Maule, C.F., Van Meijgaard, E., Panitz, H.J., Scinocca, J.F., Somot, S., 2018. The effects of 1.5 and 2 degrees of global warming on Africa in the CORDEX ensemble. Environ. Res. Lett. 13 (6) https://doi.org/10.1088/1748-9326/aab1b1.
Nile Basin Initiative, 2018. What does a global average temperature rise of 1.5 and 2 degree mean for the Nile Basin? Clim. Change Proj.: Burundi. ⟨http://nileis.nilebasin.org/system/files/Bulletin_Burundi_web.pdf⟩.
Niyongabo, H., 2018. Efficient Water Use for Agricultural Production (EWUAP) Project. Best. Pract. Water Harvest. Irrig. Burundi. ⟨http://nileis.nilebasin.org/system/files/burundi_best_practices_print.pdf⟩.
Nkunzimana, A., Bi, S., Jiang, T., Weiting, W., Abro, M.I., 2019. Spatiotemporal variation of rainfall and occurrence of extreme events over Burundi during 1960 to 2010. Arab J. Geosci. 12, 176. https://doi.org/10.1007/s12517-019-4335-y.
Osima, S., Indasi, V.S., Zaroug, M., Endris, H.S., Gudoshava, M., Misiani, H.O., Nimusiima, A., Anyah, R.O., Otieno, G., Ogwang, B.A., Jain, S., Kondowe, A.L., Mwangi, E., Lennard, C., Nikulin, G., Dosio, A., 2018. Projected climate over the Greater Horn of Africa under 1.5 ˚C and 2 ˚C global warming. Environ. Res. Lett. 13 (6) https://doi.org/10.1088/1748-9326/aaba1b.
Phoon, S.Y., Shamseldin, A.Y., Vairavamoorthy, K., 2004. Assessing impacts of climate change on Lake Victoria Basin, Africa. People-Cent. Approaches Water Environ. Sanit.: Proc. 30th WEDC Conf. 392–397.
Saeed, F., Haensler, A., Weber, T., Hagemann, S., Jacob, D., 2013. Representation of extreme precipitation events leading to opposite climate change signals over the Congo basin. Atmosphere 4 (3), 254–271. https://doi.org/10.3390/atmos4030254.
Sene, K.J., Tate, E.L., Farquharson, F.A.K., 2001. Sensitivity Studies of the Impacts of Climate Change on White Nile Flows. Clim. Change 50, 177–208. https://doi.org/10.1023/A:1010693129672.
Ogiramoi Nyeko, P.. PhD dissertation. Climate change impacts on hydrological extremes and water resources in Lake Victoria catchments, upper Nile basin. https://lirias.kuleuven.be/bitstream/123456789/319174/1//Ogiramoi_PhD_desertation_np.pdf.
Simone, D.P., Bagarello, V., and Provenzano, G., Meteorological data of Burundi, October 2007. ⟨http://climateofburundi.altervista.org⟩. Last accessed, March 2022.
Souverijns, N., Thiery, W., Demuzere, M., Lipzig, N.P.M.V., 2016. Drivers of future changes in East African precipitation. Environ. Res. Lett. 11 (11) https://doi.org/10.1088/1748-9326/11/11/114011.
Sunzu Ntigambirizwa, I.S., & Ngenzebuhoro, E., 2009, Étude de Vulnérabilité et d'adaptation aux Changements Climatique - Document de Synthése. Ministére de l'Eau, de l'Environnement, de l'Aménagement du Territoire et de l'Urbanisme; Programme des Nations Unies pour le Développement - PNUD, Bujumbura, Burundi, August 2009.
Thiery, W., Davin, E.L., Panitz, H.J., Demuzere, M., Lhermitte, S., Van Lipzig, N., 2015. The impact of the African Great Lakes on the regional climate. J. Clim. 28 (10), 4061–4085. https://doi.org/10.1175/JCLI-D-14-00565.1.
Thiery, W., Davin, E.L., Seneviratne, S.I., Bedka, K., Lhermitte, S., Van Lipzig, N.P.M., 2016. Hazardous thunderstorm intensification over Lake Victoria. Nat. Commun. 7, 1–7. https://doi.org/10.1038/ncomms12786.
Tierney, J.E., Mayes, M.T., Meyer, N., Johnson, C., Swarzenski, P.W., Cohen, A.S., Russell, J.M., 2010. Late-twentieth-century warming in Lake Tanganyika unprecedented since AD 500. Nat. Geosci. 3 (6), 422–425. https://doi.org/10.1038/ngeo865.

Tungaraza, C., Elisante, E., Osewe, Palapala, P., 2012. Long-term climate impact on the Lake Victoria region influences water level fluctuation and resource availability. Environ. Sci. Environ. Sci. Environ. Sci. 2, 1717–1732.

Van Engelen, V.W.P., Verdoodt, A., and Dijkshoorn, J.A., 2006, Soil and Terrain database of Central Africa (DR Congo, Burundi and Rwanda) (SOTERCAF, version 1.0).Report 2006/07, ISRIC World Soil information, Wageningen. (available through: ⟨http://www.isric.org⟩). Last accessed, September 2015.

Vetter, T., Reinhardt, J., Flörke, M., van Griensven, A., Hattermann, F., Huang, S., Koch, H., Pechlivanidis, I.G., Plötner, S., Seidou, O., Su, B., Vervoort, R.W., Krysanova, V., 2017. Evaluation of sources of uncertainty in projected hydrological changes under climate change in 12 large-scale river basins. Clim. Change 141, 419–433. https://doi.org/10.1007/s10584-016-1794-y.

Wainwright, C.M., Marsham, J.H., Keane, R.J., Rowell, D.P., Finney, D.L., Black, E., Allan, R.P., 2019. Eastern African Paradox rainfall decline due to shorter not less intense Long Rains. Npj Clim. Atmos. Sci. 2 (1), 1–9. https://doi.org/10.1038/s41612-019-0091-7.

Weedon, G.P., Gomes, S., Viterbo, P., Shuttleworth, W.J., Blyth, E., ÖSterle, H., Adam, J.C., Bellouin, N., Boucher, O., & Best, M., 2011. Creation of the WATCH forcing data and its use to assess global and regional reference crop evaporation over land during the twentieth century. J. Hydrometeorol. 12 (5), 823–848. https://doi.org/10.1175/2011JHM1369.1.

World Bank, 2022. ⟨https://data.worldbank.org/country/burundi.⟩. Last accessed 10th June, 2022.